© 2020. Published by The Company of Biologists Ltd | Journal of Cell Science (2020) 133, jcs244392. doi:10.1242/jcs.244392

SHORT REPORT

Phosphoregulation of the cytokinetic protein Fic1 contributes to fission yeast growth polarity establishment

K. Adam Bohnert*,§, Anthony M. Rossi§, Quan-Wen Jin‡, Jun-Song Chen and Kathleen L. Gould¶

ABSTRACT

Cellular polarization underlies many facets of cell behavior, including cell growth. The rod-shaped fission yeast *Schizosaccharomyces pombe* is a well-established, genetically tractable system for studying growth polarity regulation. *S. pombe* cells elongate at their two cell tips in a cell cycle-controlled manner, transitioning from monopolar to bipolar growth in interphase when new ends established by the most recent cell division begin to extend. We previously identified cytokinesis as a critical regulator of new end growth and demonstrated that Fic1, a cytokinetic factor, is required for normal polarized growth at new ends. Here, we report that Fic1 is phosphorylated on two C-terminal residues, which are each targeted by multiple protein kinases. Endogenously expressed Fic1 phosphomutants cannot support proper bipolar growth, and the resultant defects facilitate the switch into an invasive pseudohyphal state. Thus, phosphoregulation of Fic1 links the completion of cytokinesis to the re-establishment of polarized growth in the next cell cycle. These findings broaden the scope of signaling events that contribute to regulating *S. pombe* growth polarity, underscoring that cytokinetic factors constitute relevant targets of kinases affecting new end growth.

This article has an associated First Person interview with Anthony M. Rossi, joint first author of the paper.

KEY WORDS: Fission yeast, Polarity, Phosphoregulation, Protein kinase, Contractile ring, Fic1

INTRODUCTION

Polarization is a common feature of eukaryotic and prokaryotic cells (Hu and Lutkenhaus, 1999; Miller and Johnson, 1994). Multicellular organisms couple polarization events in neighboring cells to drive key developmental processes (Moorhouse et al., 2015). In a single cell, polarization governs processes such as growth, motility and fate specification (Mortimer et al., 2008; Pham et al., 2015; Matsuoka and Masahiro, 2018).

The fission yeast *Schizosaccharomyces pombe* is a powerful model organism for studying mechanisms by which polarization is established, maintained and modified (Arellano et al., 1999; Miller and Johnson, 1994; Ottilie et al., 1995). *S. pombe* is a rod-shaped organism, with growth limited to its cell tips (Streiblova and Wolf, 1972). After cell division, elongation occurs first only at old ends inherited from mother cells. Then, at a later point, known as new end take off (NETO), cells transition to bipolar growth by also extending at new ends established by the most recent cell division (Mitchison and Nurse, 1985).

Historically, NETO was thought to be triggered when cells reached a minimal cell size and completed S-phase (Mitchison and Nurse, 1985). However, NETO also requires proper completion of cytokinesis (Bohnert and Gould, 2012). Specifically, loss of the contractile ring (CR) protein Fic1 (Roberts-Galbraith et al., 2009) leads to abnormal persistence of CR components at new ends and curbs NETO even if factors responsible for growth are properly positioned at new cell ends (Bohnert and Gould, 2012). Barriers to NETO, caused by loss of Fic1 or other late cytokinetic factors, in turn promote growth orientations that favor a dimorphic switch from a unicellular state to a more-invasive, pseudohyphal form (Bohnert and Gould, 2012).

Our growing knowledge of NETO highlights the role of protein kinases at cell tips (Arellano et al., 2002; Fujita and Misumi, 2009; Grallert et al., 2013; Kettenbach et al., 2015; Kim et al., 2003; Kume et al., 2017, 2011; Martin et al., 2005). Polarity kinases also target CR proteins and influence their localization and cytokinetic function (Bhattacharjee et al., 2020; Lee et al., 2018; Magliozzi et al., 2020). The interplay between the fidelity of cytokinesis and proper polarity establishment in the next cell cycle, demonstrated by the role of Fic1, may therefore be phosphoregulated.

Here, we show that Fic1 is phosphorylated at two C-terminal residues. Although Cdk1 and the casein kinase II Orb5 each phosphorylate one of the sites *in vitro*, we found that none of the 111 *S. pombe* protein kinases are solely responsible for phosphorylation of either site. Fic1 phospho-mimetic and phospho-ablating mutations impaired *S. pombe* NETO and produced an invasive pseudohyphal phenotype, indicating phosphorylation controls its role in polarity. Our findings predict complex regulation of cytokinesis-based polarity determinants and suggest at least two different groups of kinases influence polarity by modulating the Fic1 phosphostate.

RESULTS AND DISCUSSION

Fic1 phosphorylation is invariant through the cell cycle

As shown previously (Bohnert and Gould, 2012), immunoblotting of Fic1–$FLAG_3$ immunoprecipitates revealed four distinct bands from untreated cells, but only one band when immunoprecipitates were treated with phosphatase (Fig. 1A). Thus, Fic1 is a phosphoprotein, and, given the multiple Fic1–$FLAG_3$ species, we conclude that Fic1 is phosphorylated on multiple residues.

To assess whether Fic1 phosphostatus is cell cycle regulated, we analyzed Fic1–$FLAG_3$ gel mobility after cell cycle arrests at different points, either through the use of temperature-sensitive

Department of Cell and Developmental Biology, Vanderbilt University School of Medicine, Nashville, TN 37240, USA.
*Present address: Department of Biological Sciences, Louisiana State University, Baton Rouge, LA 70803, USA. ‡Present address: State Key Laboratory of Cellular Stress Biology, School of Life Sciences, Xiamen University, Xiamen, Fujian 361102, China. §These authors contributed equally to this work

¶Author for correspondence (kathy.gould@vanderbilt.edu)

A.M.R., 0000-0003-3787-8573; K.L.G., 0000-0002-3810-4070

Handling Editor: David Glover
Received 21 January 2020; Accepted 12 August 2020

Journal of Cell Science (2020) 133, jcs244392. doi:10.1242/jcs.244392

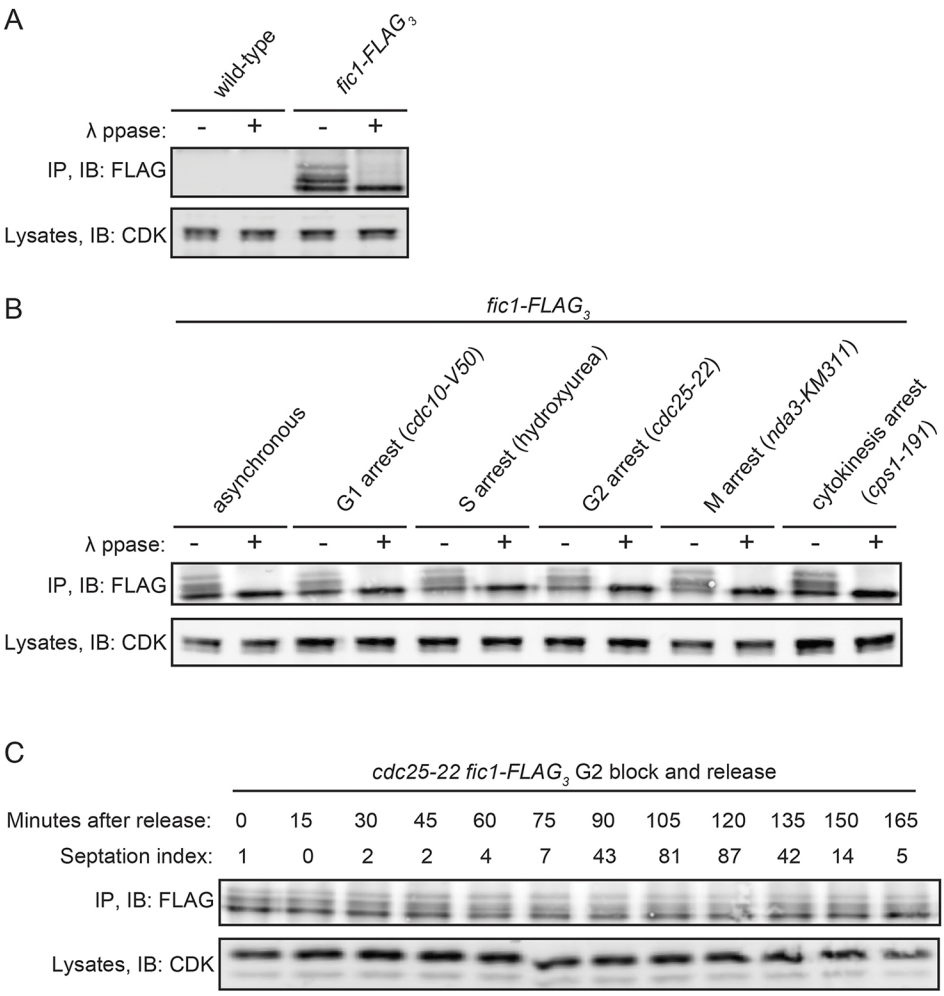

Fig. 1. Fic1 is phosphorylated *in vivo*. (A–C) Anti-FLAG immunoprecipitates (IP) from cells of indicated genotypes (A), cell cycle arrests (B) or from *cdc25-22 fic1-FLAG*$_3$ cells following release from a G2 arrest (C) were treated with lambda phosphatase (λ ppase) or vehicle and subsequently blotted (IB) with an anti-FLAG antibody. Lysate samples were blotted with anti-CDK (PSTAIRE) as a control for input into the immunoprecipitations.

alleles (*cdc10-V50* G1 arrest, *cdc25-22* G2 arrest, *nda3-KM311* prometaphase arrest, or *cps1-191* cytokinesis arrest) or after addition of hydroxyurea (S-phase arrest). In all cases, Fic1–FLAG$_3$ gel mobilities were identical (Fig. 1B). We corroborated this result using a *cdc25-22* block-and-release experiment, in which samples were taken following release from a G2 arrest. Fic1–FLAG$_3$ gel mobility shifts were identical at each time point (Fig. 1C), verifying that multiple phospho-species of Fic1 exist throughout the cell cycle.

Fic1 phosphorylation is independent of cell tip localization

The C-terminus of Fic1 (amino acids 127–end, 'Fic1C'; Fig. 2A) localizes to the CR but not to cell tips, and this fragment is necessary and sufficient for NETO (Bohnert and Gould, 2012). In contrast, the N-terminal C2 domain (amino acids 1–126, 'Fic1N'; Fig. 2A) neither localizes to the CR nor contributes to bipolar growth establishment, but is required for anchoring Fic1 to cell tips (Bohnert and Gould, 2012). Whereas Fic1N–GFP did not migrate as multiple species on SDS-PAGE gels (Fig. 2B), Fic1C–GFP showed a phosphoshift that was abrogated by phosphatase treatment (Fig. 2C). These results suggested that Fic1 phosphorylation might affect its function at the CR and, therefore, in NETO.

If this were the case, we expected that Fic1 phosphorylation would occur even if Fic1 lost its ability to anchor at cell tips. Based on homology to *S. cerevisiae* Inn1 (Devrekanli et al., 2012; Sanchez-Diaz et al., 2008), we predicted that two lysine residues within the C2 domain (Fig. 2A) mediate cell-tip localization, and we mutated them to alanine residues. Cell tip localization of Fic1-K22A,K27A–GFP was greatly reduced compared to that of Fic1–GFP (Fig. 2D,E). Additionally, whereas wild-type Fic1-GFP localized broadly across cell tips, Fic1-K22A,K27A–GFP localization at cell tips was restricted to puncta that also contained Cdc15–mCherry, a tip protein and Fic1 interactor (Roberts-Galbraith et al., 2009) (Fig. 2D,E). However, Fic1-K22A,K27A promoted proper bipolar growth (Fig. 2F–H), targeted to the CR (Fig. 2I), and was phosphorylated to the same extent as wild-type Fic1 (Fig. 2J), consistent with the idea that Fic1 phosphorylation influences its function at the CR to modulate polarity.

Fic1 is phosphorylated on two C-terminal residues

Fic1 phosphorylation sites have not been identified in proteome-wide screens (Lock et al., 2019). Thus, we used mass spectrometry of tandem affinity-purified Fic1–TAP to identify phosphorylation sites in a targeted manner. Phosphorylation of two C-terminal residues, T178 and S241, was identified (Fig. 3A,B; Fig. S1A). T178 and S241 were each mutated to alanine to abolish phosphorylation, or to aspartate to potentially mimic constitutive phosphorylation. These phosphomutants were then integrated at the endogenous *fic1* locus, tagged with FLAG$_3$, and tested for alteration in SDS-PAGE mobility. Alanine mutations of T178 or S241 individually eliminated two of the four bands, indicating that one

Journal of Cell Science (2020) 133, jcs244392. doi:10.1242/jcs.244392

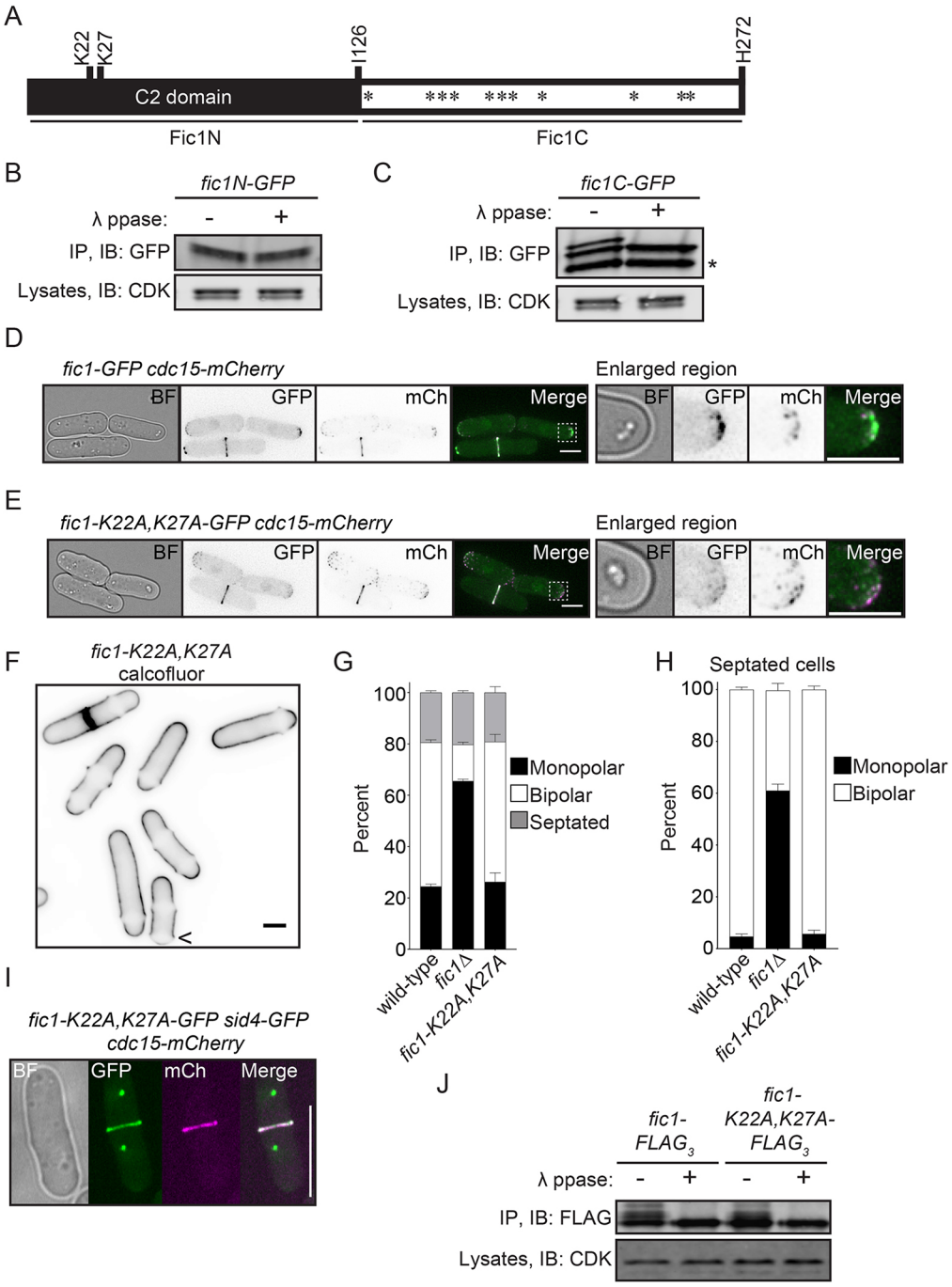

Fig. 2. Phosphorylation occurs on the region and subpopulation of Fic1 relevant to growth polarity. (A) Schematic of Fic1, drawn to scale, with residues of interest, fragments and PxxP motifs (*) indicated. (B,C) Anti-GFP immunoprecipitates from *fic1N-GFP* (B) and *fic1C-GFP* cells (C) were either treated with lambda phosphatase (λ ppase) or vehicle and subsequently blotted with an anti-GFP antibody. Lysate samples were blotted (IB) with anti-CDK (PSTAIRE) as a control for input into the immunoprecipitations (IP). An asterisk (*) indicates degradation products. (D,E) Live-cell bright field (BF), GFP, mCherry (mCh) and merged GFP/mCh images of *fic1-GFP cdc15-mCh* (D) and *fic1-K22A,K27A-GFP cdc15-mCh* (E) cells. ROIs are enlarged on the right. Scale bars: 5 µm. (F) Live-cell image of Calcofluor-stained *fic1-K22A,K27A* cells. Arrowhead indicates a monopolar cell. Scale bar: 5 µm. (G) Quantification of growth polarity phenotypes for cells of the indicated genotypes. Data from three trials per genotype with n>200 for each trial are presented as mean ±s.e.m. (H) Quantification of growth polarity phenotypes for septated cells of the indicated genotypes. Data from three trials per genotype with n>200 for each trial are presented as mean± s.e.m. (I) Live-cell BF, GFP, mCh and merged GFP/mCh images of a *fic1-K22A,K27A-GFP sid4-GFP cdc15-mCh* cell during cytokinesis. Scale bar: 10 µm. (J) Anti-FLAG immunoprecipitates from *fic1-FLAG*$_3$ and *fic1-K22A,K27A-FLAG*$_3$ cells as in Fig. 1.

band, the upper band, represented dually phosphorylated protein and each intermediate band represented singly phosphorylated Fic1 (Fig. 3C), also confirming that these two residues are the major Fic1 phosphosites. Consistent with this interpretation, Fic1-T178A, S241A (Fic1-2A) migrated as a single band (Fig. 3C). In Fic1 aspartate mutants, similar gel mobility patterns were observed, except that all bands were slightly retarded in mobility (Fig. 3C). Thus, phosphorylation occurs individually and in combination at T178 and S241 *in vivo*.

Multiple kinases modulate polarity-relevant Fic1 phosphorylation

Because phosphorylation occurs in Fic1C, which is important for polarity establishment, we set out to identify the kinase(s) responsible. T178 and S241 fit the consensus sequences for CDK (S/T-P) and CK2 (S-X-X-E/D), respectively (Fig. 3B) (Meggio et al., 1994; Nigg, 1993), and these kinases are important for polarized growth (Adams et al., 1990; McCusker et al., 2007; Rethinaswamy et al., 1998; Shimada et al., 2000; Snell and Nurse, 1994). *In vitro* kinase assays using Cdk1–cyclinB, *S. pombe* CK2 (Orb5) or human CK2 with His_6–Fic1, His_6–Fic1-T178A, and/or His_6–Fic1-S241A revealed that they can phosphorylate the sites that fit their consensus sequence (Fig. 3D,E). His_6–Fic1-T178A phosphorylation by Cdk1 was significantly reduced compared to that of His_6–Fic1, demonstrating that *in vitro* Cdk1 primarily targets T178 (Fig. 3D). To test whether Cdk1 and Orb5 phosphorylate Fic1 *in vivo*, we assayed the Fic1 phosphostatus in analog-sensitive and temperature-sensitive mutants of these kinases. The phosphostate of

Journal of Cell Science (2020) 133, jcs244392. doi:10.1242/jcs.244392

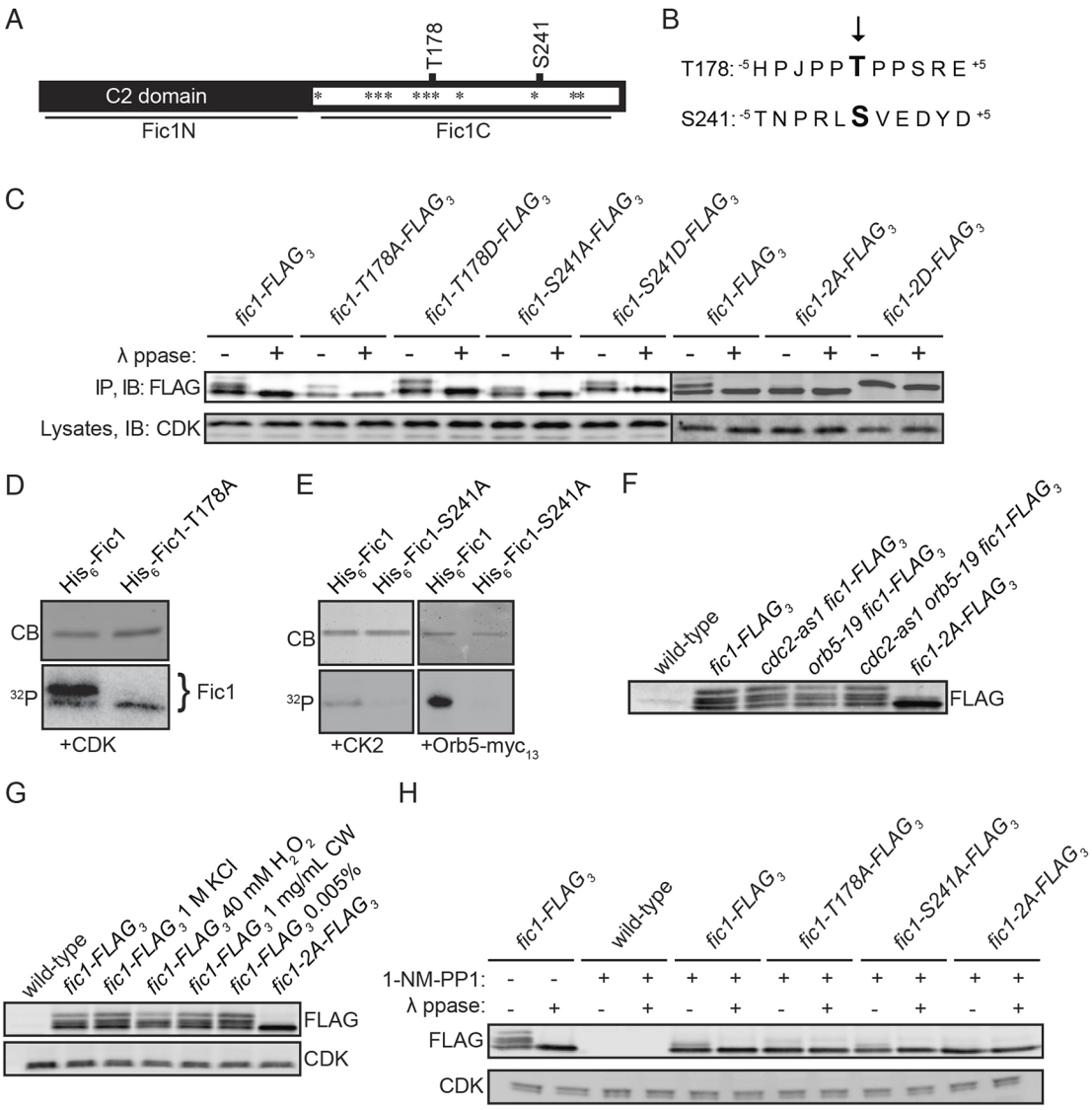

Fig. 3. Identification of Fic1 phosphorylation sites and potential kinases. (A) Schematic of Fic1. PxxP motifs (*) and phosphosites (labeled above) are indicated. (B) Schematic of Fic1 phosphosites. The phosphorylated residues are in bold text and marked by an arrow. (C) Anti-FLAG immunoprecipitates (IP) from asynchronous cells producing the indicated Fic1 proteins were either treated with lambda phosphatase (λ ppase) or vehicle and subsequently blotted (IB) with an anti-FLAG antibody. Lysate samples were blotted with anti-CDK (PSTAIRE) as a control for input into the immunoprecipitation. (D) CDK *in vitro* kinase assay using His_6–Fic1 and His_6–Fic1-T178A. (E) CK2 *in vitro* kinase assay using His_6–Fic1 and His_6—Fic1-S241A. (D,E) Protein labeled by γ-[^{32}P]ATP was detected by autoradiography, and the gel was stained with Coomassie Blue as a loading control. (F) Lysates from cells of the indicated genotypes were immunoblotted with anti-FLAG antibody to assess Fic1–$FLAG_3$ gel mobilities. For *orb5-19* strains, cells were shifted to 36°C for 4 h prior to lysis. For *cdc2-as1* strains, cells were treated with 1 µM of 1-NM-PP1 for 30 min prior to lysis. (G) Lysates from cells of the indicated genotypes were immunoblotted with anti-FLAG antibody to assess Fic1–$FLAG_3$ gel mobilities after 60 min in 1 M KCl, 1 mg/ml Calcofluor, or 0.005% SDS or 15 min in 40 mM H_2O_2. Lysates were immunoblotted with anti-CDK (PSTAIRE) as a loading control. (H) Anti-FLAG immunoprecipitates from cells of indicated genotypes that had been treated with 50 µM of 1-NM-PP1 for 30 min before lysis were treated with lambda phosphatase or vehicle, and subsequently blotted with an anti-FLAG antibody. Lysate samples were blotted with anti-CDK (PSTAIRE) as a control for input into the immunoprecipitations.

Fic1 was unaltered in these single and double mutants (Fig. 3F). Thus, Cdk1 and Orb5 are not solely responsible for Fic1 phosphorylation *in vivo*.

We next took an unbiased approach to try to identify the kinase(s) responsible for Fic1 phosphorylation. Starting with polarity kinases, then extending to all kinases, we screened gene deletions of individual non-essential kinases, temperature or analog-sensitive mutants of essential protein kinase genes, and combination mutants of paralogs (e.g. *pck1-as pck2-as*) for changes to the phosphostate of Fic1 (Bimbó et al., 2005; Chen et al., 2014; Cipak et al., 2011; Gregan et al., 2007; Kim et al., 2010). In the course of this screening, we determined that several kinase deletion strains in Bioneer V3 (Kim et al., 2010) contained not only a targeted deletion allele but also the wild-type kinase gene. Thus, we constructed new deletion mutants of *atg1*, *hal4*, *lsk1*, *mak2*, *mek1*, *sty1*, *ppk24*, *ppk34* and *wis1*. Through immunoblotting, we did not detect loss of either Fic1 phosphorylation event in any of the 111 single or 11 combination kinase mutants tested (Figs S1B and S2), indicating that multiple kinases can phosphorylate Fic1.

We next tried to identify pathways regulating the Fic1 phosphostate. To this end, we treated cells with osmotic, oxidative, cell wall integrity, and plasma membrane stressors

(Cadou et al., 2010; Chen et al., 2008; Madrid et al., 2006; Robertson and Hagan, 2008). None of the stressors tested evoked a change in the phosphostate of Fic1 (Fig. 3G). However, phosphorylation at S241, but not T178, was lost after treatment with a high dose of 1-NM-PP1 (Fig. 3H). 1-NM-PP1 is an inhibitor designed to preferentially target kinases with space-creating mutations in their ATP-binding pocket. However, some kinase families such as Src, CDK and CAMKII, are sensitive to high levels of 1-NM-PP1 (Bishop et al., 2000). Loss of phosphorylation on S241 but not on T178 suggests that distinct groups of kinases phosphorylate each site, one of which can be inhibited by high levels of 1-NM-PP1. Collectively, these data establish that Fic1 phosphoregulation involves multiple kinases that are apparently coordinated to keep the ratios of Fic1 phosphorylation events similar throughout the cell cycle and under different physiological conditions.

Fic1 phosphorylation does not affect CR localization or interaction with known CR-binding partners

To assess whether disrupting the phosphorylation state of Fic1 altered its localization, we analyzed the fluorescence intensities of mNeonGreen-tagged Fic1 variants at the CR and cell tips. We observed no differences between Fic1 and the Fic1 phosphomutants (Fig. 4A,B). Next, we performed time-lapse imaging to determine whether Fic1 CR recruitment timing relative to spindle pole body (SPB) separation differed for either phosphomutant. We found that Fic1, Fic1-2A, and Fic1-2D were recruited to the CR with similar timing (Fig. 4C).

Fic1 localizes to the CR via its interaction with the SH3 domains of the F-BAR proteins, Cdc15 and Imp2 (Roberts-Galbraith et al., 2009; Ren et al., 2015). Because one Fic1 phosphosite (S241) is proximal to the P254-P257 PxxP motif required for these SH3 domain interactions (Bohnert and Gould, 2012), we tested whether phosphorylation interferes with Cdc15 and Imp2 binding. Consistent with normal CR recruitment, both Fic1 phosphomutants co-immunoprecipitated with Cdc15 and Imp2 (Fig. S3A), indicating that deregulation of Fic1 phosphorylation does not grossly alter these known interactions.

Disruption of Fic1 phosphorylation impacts bipolar cell growth and promotes pseudohyphal growth

To assess the relevance of Fic1 phosphorylation to NETO, we analyzed the growth polarity of the phosphomutants (Fig. 4D). *fic1-2A* and *fic1-2D* had similar levels of monopolar cells to those in *fic1*Δ, whereas each individual phosphomutant displayed levels that were intermediate between wild type and *fic1*Δ (Fig. 4D–F). Also, as expected given that wild-type cells commonly initiate NETO by late interphase, nearly all *fic1*$^{+}$ cells arrested in late G2 exhibited bipolar growth (Fig. S3B,C). In contrast, a high percentage of *cdc25-22 fic1-2A* and *cdc25-22 fic1-2D* cells were still monopolar, like *cdc25-22 fic1*Δ (Fig. S3B,C). By using time-lapse DIC imaging, we confirmed that the polarized growth defects in *fic1*Δ, *fic1-2A* and *fic1-2D* were specific to new ends (Fig. 4G; Fig. S3D). Although the phosphomutants did not support proper NETO, they retained some function because they are not synthetically lethal with *pxl1*Δ, *ppb1*Δ or *sid2-250* like *fic1*Δ (Bohnert and Gould, 2012) (Fig. S3E), possibly because they can still associate with Cdc15 and Imp2 (Fig. S3A). Considering our results together, we hypothesize that phosphorylation affects the interaction of Fic1 with unknown factor(s) at the CR that influences its CR function.

Inability to support proper NETO is exhibited by *S. pombe* and *S. japonicus* cells that have undergone the dimorphic switch from single-celled to pseudohyphal growth (Dodgson et al., 2010; Sipiczki et al., 1998), and *fic1*Δ cells show increased invasive pseudoyhyphal growth compared to that shown by wild-type cells (Fig. 4H,I; Fig. S3F) (Bohnert and Gould, 2012). Consistent with *fic1* phosphomutants possessing growth polarity defects akin to *fic1*Δ, *fic1-2A* and *fic1-2D* cells formed pseudohyphal structures invading the agar (Fig. 4H; Fig. S3F,G). Also, each individual Fic1 aspartate mutant was more invasive than wild-type (Fig. S3F). Thus, the dimorphic switch from single-celled to pseudohyphal form may involve Fic1 phosphoregulation.

In conclusion, although phosphorylation serves diverse roles during eukaryotic cytokinesis (Bohnert and Gould, 2011), it has been unclear whether CR protein phosphorylation impacts cellular processes other than cell division. In this study, we found that Fic1 phosphorylation influences polarity and the transition to hyphal growth. Our findings support the ideas that (1) regulating CR function can directly impact the dimorphic switch; and (2) modulation of kinase and/or phosphatase signaling may be sufficient for this switch. As extensive phosphosignaling occurs during hyphal growth (Sudbery, 2011), integration of multiple cues likely guarantees the robustness of this transition.

MATERIALS AND METHODS

Yeast methods

S. pombe strains (Table S1) were grown in yeast extract with supplements (YES) or Edinburgh minimal medium with relevant supplements. Genes were tagged at the 3′ end of their ORFs with sequences encoding GFP:kan^{R}, HA$_3$:hyg^{R}, FLAG$_3$:kan^{R}, mNeonGreen:kanR or FLAG$_3$:hyg^{R} using pFA6 cassettes as previously described (Bähler et al., 1998; Wach et al., 1994). A lithium acetate method (Keeney and Boeke, 1994) was used in *S. pombe* tagging transformations, and integration of tags was verified using whole-cell PCR and/or microscopy. Introduction of tagged loci into other genetic backgrounds was accomplished using standard *S. pombe* mating, sporulation and tetrad dissection techniques. For arresting *cdc25-22* and *cps1-191*, cells were grown at 25°C and then shifted to 36°C for 3 h. *nda3-KM311* arrest was achieved by growing cells at 32°C and then shifting to 18°C for 6.5 h. For blocking of *cdc10-V50*, cells were grown at 25°C and then shifted to 36°C for 4 h. S-phase arrest was achieved by treating cells with 12 mM hydroxyurea for 4 h at 32°C.

Mutants and truncations of *fic1* were expressed from the endogenous *fic1*$^{+}$ locus. To make these strains, a pIRT2 vector was used in which *fic1*$^{+}$ gDNA with 5′ and 3′ flanks was inserted between BamHI and PstI sites of pIRT2 (Bohnert and Gould, 2012). Mutations were then introduced via site-directed mutagenesis and confirmed by DNA sequencing. *fic1*Δ was transformed with these pIRT2-*fic1* constructs, and stable integrants resistant to 1.5 g/l 5-fluoroorotic acid (5-FOA) were isolated and confirmed by whole-cell PCR, DNA sequencing and immunoblotting.

To construct analog-sensitive protein kinase strains, the coding sequences with 5′ and 3′ flanks of *pck1*$^{+}$, *pck2*$^{+}$ and *nnk1*$^{+}$ were PCR amplified from *S. pombe* genomic DNA using PrimeSTAR GXL DNA polymerase (Takara) and ligated into the pCR-Blunt II-TOPO® vector (Invitrogen). The resulting inserts were verified by sequencing. The gate-keeper residues in Pck1 and Pck2 kinases were identified as M744 and M763, respectively, and in Nnk1 kinase as M537 (Gregan et al., 2007). These residues were mutated to glycine or alanine using mutagenic oligonucleotide primers and QuikChange II site-directed mutagenesis kit (Stratagene). The desired mutations were verified by sequencing. Next the *pck1*- and *pck2*-containing plasmids were linearized and transformed into *pck1::ura4*$^{+}$ and *pck1::ura4*$^{+}$ cells, respectively, and the plasmids containing *nnk1-as* mutations were transformed into *nnk1::ura4*$^{+}$-*HA$_3$-TAP:kan^{R}* P_{nmt41}-GBP-mCherry-*nnk1-leu1*$^{+}$, using a lithium acetate method (Keeney and Boeke, 1994). Transformants were selected based on resistance to 5-FOA and then confirmed first by colony PCR and then by DNA sequencing. Next, the allele P_{nmt41}-GBP-mCherry-*nnk1-leu1*$^{+}$ was crossed out to obtain *nnk1(M537G)-HA$_3$-TAP:kan^{R}* and *nnk1(M537A)-HA$_3$-TAP:kan^{R}*.

For serial-dilution growth assays, cells were grown in liquid YE at 32°C; then, three serial 1:10 dilutions starting at 4×10^{6} were created, 2 µl of each

Journal of Cell Science (2020) 133, jcs244392. doi:10.1242/jcs.244392

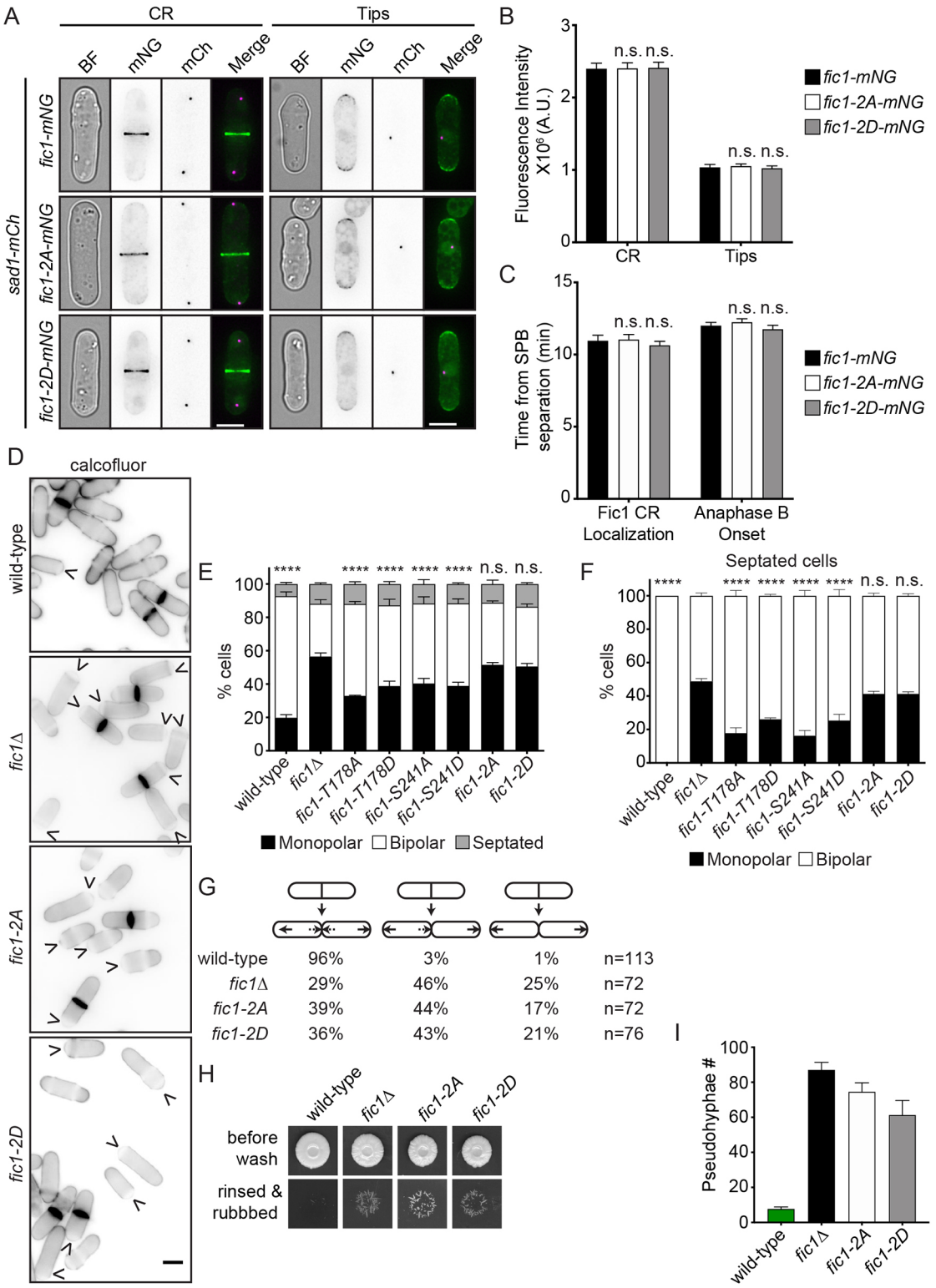

Fig. 4. Deregulation of Fic1 phosphorylation at T178 an S241 impairs new end growth. (A) Live-cell bright field (BF), GFP, mCherry (mCh) and merged GFP/mCh images of cells of indicated genotypes during cytokinesis and interphase. Scale bars: 5 µm. (B) Quantification of fluorescence intensities of CR and cell tips for cells of indicated genotypes. Data from three trials per genotype with n=15 for each trial are presented as mean±s.e.m. (C) Quantification from time-lapse imaging for cells of indicated genotypes. Data from two trials n=25 are presented as mean±s.e.m. (B,C) Analyzed by two-way ANOVA; n.s., not significant. (D) Live-cell images of calcofluor-stained cells of the indicated genotypes. Arrowheads indicate monopolar cells. (E,F) Quantification of growth polarity phenotypes for cells (E) and septated cells (F) of the indicated genotypes. Data from three trials per genotype with n>200 for each trial are presented as mean ±s.e.m. The percentage of monopolar cells between *fic1*Δ and each other genotype was compared. ****P<0.0001, n.s., not significant (two-way ANOVA with Dunnett's multiple-comparisons test). (G) Quantification of growth patterns for cells of the indicated genotypes. (H) Invasive growth assays for strains of the indicated genotypes on 2% agar. Cells were spotted on rich medium and incubated for 20 days at 29°C (top panel). Colonies were then rinsed under a stream of water and rubbed off (bottom panel). (I) Quantification (mean±s.e.m.) of pseudohyphae for cells of the indicated genotypes, with n≥3 spots counted for each genotype.

dilution was spotted on YE agar and cells were grown at the indicated temperatures for 3–5 days.

Protein methods

Cells were lysed by bead disruption in NP40 lysis buffer in denaturing conditions as previously described (Gould et al., 1991), except with the addition of 0.5 mM diisopropyl fluorophosphate (Sigma-Aldrich). Immunoblot analysis of cell lysates and immunoprecipitates was performed using anti-FLAG (M2; Sigma-Aldrich; 1:5000; cat. no. F1804) or anti-PSTAIRE Cdc2 (Sigma-Aldrich; 1:5000; cat. no. P7962) antibodies or serums raised against GST-Cdc15 (VU326; 1:2000) (Roberts-Galbraith et al., 2009) or His_6-Imp2 (VU483; 1:1000) (McDonald et al., 2016) as previously described (Bohnert et al., 2009). For gel shifts, denatured samples were treated with lambda-phosphatase (New England Biolabs) in 25 mM HEPES-NaOH (pH 7.4), 150 mM NaCl, and 1 mM $MnCl_2$ and incubated for 30 min at 30°C with shaking.

In vitro kinase assays with kinase-active Cdk1 were performed as described by Yoon et al. (2006) using a kinase buffer consisting of 50 mM Tris-HCl pH 7.4, 10 mM $MgCl_2$ and 2 mM DTT supplemented with 10 µM cold ATP and 5 µCi γ-[^{32}P]ATP. Reactions contained 100 ng of kinase-active Cdk1 and 1 µg of recombinant His_6–Fic1, His_6–Fic1–T178A or His_6–Fic1-S241A. The addition of sample buffer and boiling terminated the reactions. Samples of each reaction were separated by SDS-PAGE and visualized by Coomassie Blue staining and autoradiography.

Mass spectrometry analysis

Tandem affinity purifications (TAPs) for Fic1–TAP proteins were conducted as described previously (Gould et al., 2004). Proteins were subjected to mass spectrometric analysis on an LTQ Velos by 3-phase multidimensional protein identification technology, as previously described (McDonald et al., 2002; Chen et. al., 2013) with modifications. Proteins were resuspended in 8 M urea buffer (8 M urea in 100 mM Tris-HCl, pH 8.5), reduced with Tris (2-carboxyethyl) phosphine, alkylated with 2-chloro acetamide, and digested with trypsin or chymotrypsin. The resulting peptides were desalted by C-18 spin column (Pierce). Raw mass spectrometry data were filtered with Scansifter and searched by SEQUEST algorithm. Scaffold (version 4.4.8 or version 4.2.1) and Scaffold PTM (version 3.0.1) (both from Proteome Software, Portland, OR) were used for data assembly and filtering. Phosphorylation sites were filtered to 50% Scaffold localization using Scaffold PTM (v2.0, Proteome Software, Portland, OR) and Ascores (Beausoleil et al., 2006).

Microscopy

Live-cell images of *S. pombe* were acquired using one of the following: (1) a spinning disc confocal microscope (Ultraview LCI, PerkinElmer) equipped with a 100× NA 1.40 PlanApo oil immersion objective, a 488-nm argon ion laser (GFP and mNeonGreen), a 594-nm helium neon laser (mCherry), a charge-coupled device camera (Orca-ER, Hamamatsu Phototonics), and Metamorph 7.1 software (MDS Analytical Technologies and Molecular Devices) or (2) a personal DeltaVision microscope system (Applied Precision) that includes an Olympus IX71 microscope, 60× NA 1.42 PlanApo and 100× NA 1.40 UPlanSApo objectives, a Photometrics CoolSnap HQ2 camera, and softWoRx imaging software. All cells were in log phase growth before temperature-sensitive shifts and/or live imaging.

For Calcofluor staining, cells were washed in PBS and then resuspended in PBS containing 5 µg/ml Calcofluor. After incubation on ice for 30 min, cells were washed three times in PBS and images were acquired. Using the proximity of birth scars to cell ends, growth/morphology was scored as one of the following: monopolar (i.e. growth on one end), bipolar (i.e. growth on both ends), monopolar and septated, bipolar and septated, or multiseptated. For cells just completing division, daughter cells were scored as monopolar as long as ingression of the mother cell had progressed to such a degree that birth scars could be easily identified at new ends. All cells stained with Calcofluor were grown to log phase at 25°C, except that *cdc25-22* mutants were grown overnight at 25°C and then shifted to 36°C for 3 h before staining.

Intensity measurements were made with ImageJ software (Schindelin et al., 2012) using non-deconvolved summed *Z*-projections of the images. For all intensity measurements, the background was subtracted by creating a region of interest (ROI) in the same image in an area clear of cells. The background raw intensity was divided by the area of the background, which was multiplied by the area of the ROI. This number was subtracted from the raw integrated intensity of that ROI. To account for autofluorescence, cells lacking fluorescent tags but otherwise of isogenic backgrounds, were imaged and the fluorescence intensity per pixel was quantified from summed *Z*-projections of the images by subtracting the background intensity from the measured raw integrated intensity of the ROI before dividing the raw integrated intensity of the ROI by the area of that ROI. This autofluorescence per pixel measurement was multiplied by the area of the ROI from fluorescent cells before subtracting this value from the from the raw integrated intensity of that ROI. Representative images are max intensity *Z*-projections.

Time-lapse imaging was performed using an ONIX microfluidics perfusion system (CellASIC ONIX; EMD Millipore). A suspension of 50 µl of 40×10^6 cells/ml YE was loaded into Y04C plates for 5 s at 8 psi. YE medium was flowed through the chamber at 5 psi throughout imaging.

Images of yeast cells and pseudohyphae on YE agar plates were acquired by focusing a camera (PowerShot SD750; Canon) through a microscope (Universal; Carl Zeiss) equipped with a 20× NA 0.32 objective.

Invasive growth assays

To assay pseudohyphal invasion into 2% agar, 5 µl containing a total of 10^5 cells were spotted on 2% YE agar and incubated at 29°C for 20 days. Colonies were subsequently placed under a steady stream of water, and surface growth was wiped off using a paper towel, as described previously (Pöhlmann and Fleig, 2010; Prevorovsky et al., 2009).

Acknowledgements

We thank Alaina Willet, Sierra Cullati, and Chloe Snider for critical reading of the manuscript and Malwina Huzarska for technical assistance. Some data in the paper formed part of Kenneth Adam Bohnert's PhD thesis in the Department of Cell and Developmental Biology at Vanderbilt University in 2013.

Competing interests

The authors declare no competing or financial interests.

Author contributions

Conceptualization: K.L.G., K.A.B., A.M.R.; Methodology: K.L.G., K.A.B., A.M.R., Q.-W.J., J.-S.C.; Software: J.-S.C.; Validation: K.L.G., K.A.B., A.M.R., Q.-W.J., J.-S.C.; Formal analysis: K.A.B., A.M.R., Q.-W.J., J.-S.C.; Investigation: K.A.B., A.M.R., Q.-W.J., J.-S.C.; Resources: K.L.G.; Data curation: K.L.G., A.M.R., Q.-W.J., J.-S.C.; Writing - original draft: K.L.G., K.A.B., A.M.R.; Writing - review & editing: K.L.G., K.A.B., A.M.R., Q.-W.J., J.-S.C.; Visualization: K.A.B., A.M.R.; Supervision: K.L.G.; Project administration: K.L.G.; Funding acquisition: K.L.G.

Funding

K.A.B. was supported by National Institutes of Health (NIH) grant T32 CA119925, and A.M.R. was supported by NIH grant T32 GM008554. This work was supported by NIGMS grants R01 GM101035 and R35 GM131799 to K.L.G. Deposited in PMC for release after 12 months.

Supplementary information

Supplementary information available online at
https://jcs.biologists.org/lookup/doi/10.1242/jcs.244392.supplemental

References

Adams, A. E., Johnson, D. I., Longnecker, R. M., Sloat, B. F. and Pringle, J. R. (1990). CDC42 and CDC43, two additional genes involved in budding and the establishment of cell polarity in the yeast Saccharomyces cerevisiae. *J. Cell Biol.* **111**, 131-142. doi:10.1083/jcb.111.1.131

Arellano, M., Coll, P. M. and Pérez, P. (1999). RHO GTPases in the control of cell morphology, cell polarity, and actin localization in fission yeast. *Microsc. Res. Tech.* **47**, 51-60. doi:10.1002/(SICI)1097-0029(19991001)47:1<51::AID-JEMT5>3.0.CO;2-3

Arellano, M., Niccoli, T. and Nurse, P. (2002). Tea3p is a cell end marker activating polarized growth in Schizosaccharomyces pombe. *Curr. Biol.* **12**, 751-756. doi:10.1016/S0960-9822(02)00821-7

Bähler, J., Wu, J.-Q., Longtine, M. S., Shah, N. G., McKenzie, A., III, Steever, A. B., Wach, A., Philippsen, P. and Pringle, J. R. (1998). Heterologous modules for efficient and versatile PCR-based gene targeting in *Schizosaccharomyces*

pombe. *Yeast* **14**, 943-951. doi:10.1002/(SICI)1097-0061(199807)14:10<943::AID-YEA292>3.0.CO;2-Y

Beausoleil, S. A., Villén, J., Gerber, S. A., Rush, J. and Gygi, S. P. (2006). A probability-based approach for high-throughput protein phosphorylation analysis and site localization. *Nat. Biotechnol.* **24**, 1285-1292. doi:10.1038/nbt1240

Bhattacharjee, R., Mangione, M. C., Wos, M., Chen, J.-S., Snider, C. E., Roberts-Galbraith, R. H., McDonald, N. A., Presti, L. L., Martin, S. G. and Gould, K. L. (2020). DYRK kinase Pom1 drives F-BAR protein Cdc15 from the membrane to promote medial division. *Mol. Biol. Cell* **31**, 917-929. doi:10.1091/mbc.E20-01-0026

Bimbó, A., Jia, Y., Poh, S. L., Karuturi, R. K. M., den Elzen, N., Peng, X., Zheng, L., O'Connell, M., Liu, E. T., Balasubramanian, M. K. et al. (2005). Systematic deletion analysis of fission yeast protein kinases. *Eukaryot. Cell* **4**, 799-813. doi:10.1128/EC.4.4.799-813.2005

Bishop, A. C., Ubersax, J. A., Petsch, D. T., Matheos, D. P., Gray, N. S., Blethrow, J., Shimizu, E., Tsien, J. Z., Schultz, P. G., Rose, M. D. et al. (2000). A chemical switch for inhibitor-sensitive alleles of any protein kinase. *Nature* **407**, 395-401. doi:10.1038/35030148

Bohnert, K. A. and Gould, K. L. (2011). On the cutting edge: post-translational modifications in cytokinesis. *Trends Cell Biol.* **21**, 283-292. doi:10.1016/j.tcb.2011.01.006

Bohnert, K. A. and Gould, K. L. (2012). Cytokinesis-based constraints on polarized cell growth in fission yeast. *PLoS Genet.* **8**, e1003004. doi:10.1371/journal.pgen.1003004

Bohnert, K. A., Chen, J.-S., Clifford, D. M., Vander Kooi, C. W. and Gould, K. L. (2009). A Link between aurora kinase and Clp1/Cdc14 regulation uncovered by the identification of a fission yeast borealin-like protein. *Mol. Biol. Cell* **20**, 3646-3659. doi:10.1091/mbc.e09-04-0289

Cadou, A., Couturier, A., Le Goff, C., Soto, T., Miklos, I., Sipiczki, M., Xie, L., Paulson, J. R., Cansado, J. and Le Goff, X. (2010). Kin1 is a plasma membrane-associated kinase that regulates the cell surface in fission yeast. *Mol. Microbiol.* **77**, 1186-1202. doi:10.1111/j.1365-2958.2010.07281.x

Chen, D., Wilkinson, C. R. M., Watt, S., Penkett, C. J., Toone, W. M., Jones, N. and Bähler, J. (2008). Multiple pathways differentially regulate global oxidative stress responses in fission yeast. *Mol. Biol. Cell* **19**, 308-317. doi:10.1091/mbc.e07-08-0735

Chen, J.-S., Broadus, M. R., McLean, J. R., Feoktistova, A., Ren, L. and Gould, K. L. (2013). Comprehensive proteomics analysis reveals new substrates and regulators of the fission yeast Clp1/Cdc14 phosphatase. *Mol. Cell. Proteomics* **12**, 1074-1086. doi:10.1074/mcp.M112.025924

Chen, J.-S., Beckley, J. R., McDonald, N. A., Ren, L., Mangione, M. S., Jang, S. J., Elmore, Z. C., Rachfall, N., Feoktistova, A., Jones, C. M. et al. (2014). Identification of new players in cell division, DNA damage response, and morphogenesis through construction of Schizosaccharomyces pombe deletion strains. *G3 (Bethesda)* **5**, 361-370. doi:10.1534/g3.114.015701

Cipak, L., Zhang, C., Kovacikova, I., Rumpf, C., Miadokova, E., Shokat, K. M. and Gregan, J. (2011). Generation of a set of conditional analog-sensitive alleles of essential protein kinases in the fission yeast Schizosaccharomyces pombe. *Cell Cycle* **10**, 3527-3532. doi:10.4161/cc.10.20.17792

Devrekanli, A., Foltman, M., Roncero, C., Sanchez-Diaz, A. and Labib, K. (2012). Inn1 and Cyk3 regulate chitin synthase during cytokinesis in budding yeasts. *J. Cell Sci.* **125**, 5453-5466. doi:10.1242/jcs.109157

Dodgson, J., Brown, W., Rosa, C. A. and Armstrong, J. (2010). Reorganization of the growth pattern of Schizosaccharomyces pombe in invasive filament formation. *Eukaryot. Cell* **9**, 1788-1797. doi:10.1128/EC.00084-10

Fujita, A. and Misumi, Y. (2009). Fission yeast syt22 protein, a putative Arf guanine nucleotide exchange factor, is necessary for new end take off. *FEMS Microbiol. Lett.* **294**, 191-197. doi:10.1111/j.1574-6968.2009.01566.x

Gould, K. L., Moreno, S., Owen, D. J., Sazer, S. and Nurse, P. (1991). Phosphorylation at Thr167 is required for *Schizosaccharomyces pombe* p34cdc2 function. *EMBO J.* **10**, 3297-3309. doi:10.1002/j.1460-2075.1991.tb04894.x

Gould, K. L., Ren, L., Feoktistova, A. S., Jennings, J. L. and Link, A. J. (2004). Tandem affinity purification and identification of protein complex components. *Methods* **33**, 239-244. doi:10.1016/j.ymeth.2003.11.019

Grallert, A., Patel, A., Tallada, V. A., Chan, K. Y., Bagley, S., Krapp, A., Simanis, V. and Hagan, I. M. (2013). Centrosomal MPF triggers the mitotic and morphogenetic switches of fission yeast. *Nat. Cell Biol.* **15**, 88-95. doi:10.1038/ncb2633

Gregan, J., Zhang, C., Rumpf, C., Cipak, L., Li, Z., Uluocak, P., Nasmyth, K. and Shokat, K. M. (2007). Construction of conditional analog-sensitive kinase alleles in the fission yeast Schizosaccharomyces pombe. *Nat. Protoc.* **2**, 2996-3000. doi:10.1038/nprot.2007.447

Hu, Z. and Lutkenhaus, J. (1999). Topological regulation of cell division in Escherichia coli involves rapid pole to pole oscillation of the division inhibitor MinC under the control of MinD and MinE. *Mol. Microbiol.* **34**, 82-90. doi:10.1046/j.1365-2958.1999.01575.x

Keeney, J. B. and Boeke, J. D. (1994). Efficient targeted integration at leu1-32 and ura4-294 in *Schizosaccharomyces pombe*. *Genetics* **136**, 849-856.

Kettenbach, A. N., Deng, L., Wu, Y., Baldissard, S., Adamo, M. E., Gerber, S. A. and Moseley, J. B. (2015). Quantitative phosphoproteomics reveals pathways for coordination of cell growth and division by the conserved fission yeast kinase pom1. *Mol. Cell. Proteomics* **14**, 1275-1287. doi:10.1074/mcp.M114.045245

Kim, H. W., Yang, P., Catanuto, P., Verde, F., Lai, H., Du, H., Chang, F. and Marcus, S. (2003). The kelch repeat protein, Tea1, is a potential substrate target of the p21-activated kinase, Shk1, in the fission yeast, Schizosaccharomyces pombe. *J. Biol. Chem.* **278**, 30074-30082. doi:10.1074/jbc.M302609200

Kim, D.-U., Hayles, J., Kim, D., Wood, V., Park, H.-O., Won, M., Yoo, H.-S., Duhig, T., Nam, M., Palmer, G. et al. (2010). Analysis of a genome-wide set of gene deletions in the fission yeast Schizosaccharomyces pombe. *Nat. Biotechnol.* **28**, 617-623. doi:10.1038/nbt.1628

Kume, K., Koyano, T., Kanai, M., Toda, T. and Hirata, D. (2011). Calcineurin ensures a link between the DNA replication checkpoint and microtubule-dependent polarized growth. *Nat. Cell Biol.* **13**, 234-242. doi:10.1038/ncb2166

Kume, K., Hashimoto, T., Suzuki, M., Mizunuma, M., Toda, T. and Hirata, D. (2017). Identification of three signaling molecules required for calcineurin-dependent monopolar growth induced by the DNA replication checkpoint in fission yeast. *Biochem. Biophys. Res. Commun.* **491**, 883-889. doi:10.1016/j.bbrc.2017.07.129

Lee, M. E., Rusin, S. F., Jenkins, N., Kettenbach, A. N. and Moseley, J. B. (2018). Mechanisms connecting the conserved protein kinases Ssp1, Kin1, and Pom1 in fission yeast cell polarity and division. *Curr. Biol.* **28**, 84-92.e4. doi:10.1016/j.cub.2017.11.034

Lock, A., Rutherford, K., Harris, M. A., Hayles, J., Oliver, S. G., Bähler, J. and Wood, V. (2019). PomBase 2018: user-driven reimplementation of the fission yeast database provides rapid and intuitive access to diverse, interconnected information. *Nucleic Acids Res.* **47**, D821-D827. doi:10.1093/nar/gky961

Madrid, M., Soto, T., Khong, H. K., Franco, A., Vicente, J., Pérez, P., Gacto, M. and Cansado, J. (2006). Stress-induced response, localization, and regulation of the Pmk1 cell integrity pathway in Schizosaccharomyces pombe. *J. Biol. Chem.* **281**, 2033-2043. doi:10.1074/jbc.M506467200

Magliozzi, J. O., Sears, J., Cressey, L., Brady, M., Opalko, H. E., Kettenbach, A. N. and Moseley, J. B. (2020). Fission yeast Pak1 phosphorylates anillin-like Mid1 for spatial control of cytokinesis. *J. Cell Biol.* **219**, e201908017. doi:10.1083/jcb.201908017

Martin, S. G., McDonald, W. H., Yates, J. R., III and Chang, F. (2005). Tea4p links microtubule plus ends with the formin for3p in the establishment of cell polarity. *Dev. Cell* **8**, 479-491. doi:10.1016/j.devcel.2005.02.008

Matsuoka, S. and Masahiro, U. (2018). Mutual inihibition between PTEN and PIP3 generates bistability for polarity in motile cells. *Nat. Commun.* **9**, 4481. doi:10.1038/s41467-018-06856-0

McCusker, D., Denison, C., Anderson, S., Egelhofer, T. A., Yates, J. R., III, Gygi, S. P. and Kellogg, D. R. (2007). Cdk1 coordinates cell-surface growth with the cell cycle. *Nat. Cell Biol.* **9**, 506-515. doi:10.1038/ncb1568

McDonald, N. A., Takizawa, Y., Feoktistova, A., Xu, P., Ohi, M. D., Vander Kooi, C. W. and Gould, K. L. (2016). The tubulation activity of a fission yeast F-BAR protein is dispensable for its function in cytokinesis. *Cell Rep.* **14**, 534-546. doi:10.1016/j.celrep.2015.12.062

McDonald, W. H., Ohi, R., Miyamoto, D. T., Mitchison, T. J. and Yates, J. R. (2002). Comparison of three directly coupled HPLC MS/MS strategies for identification of proteins from complex mixtures: single-dimension LC-MS/MS, 2-phase MudPIT, and 3-phase MudPIT. *Int. J. Mass Spectrom.* **219**, 245-251. doi:10.1016/S1387-3806(02)00563-8

Meggio, F., Marin, O. and Pinna, L. A. (1994). Substrate specificity of protein kinase CK2. *Cell. Mol. Biol. Res.* **40**, 401-409.

Miller, P. J. and Johnson, D. I. (1994). Cdc42p GTPase is involved in controlling polarized cell growth in Schizosaccharomyces pombe. *Mol. Cell. Biol.* **14**, 1075-1083. doi:10.1128/MCB.14.2.1075

Mitchison, J. M. and Nurse, P. (1985). Growth in cell length in the fission yeast Schizosaccharomyces pombe. *J. Cell Sci.* **75**, 357-376.

Moorhouse, K. S., Gudejko, H. F. M., McDougall, A. and Burgess, D. R. (2015). Influence of cell polarity on early development of the sea urchin embryo. *Dev. Dyn.* **244**, 1469-1484. doi:10.1002/dvdy.24337

Mortimer, D., Fothergill, T., Pujic, Z., Richards, L. J. and Goodhill, G. J. (2008). Growth cone chemotaxis. *Trends Neurosci.* **31**, 90-98. doi:10.1016/j.tins.2007.11.008

Nigg, E. A. (1993). Cellular substrates of p34cdc2 and its companion cyclin-dependent kinases. *Trends Cell Biol.* **3**, 296-301. doi:10.1016/0962-8924(93)90011-O

Ottilie, S., Miller, P. J., Johnson, D. I., Creasy, C. L., Sells, M. A., Bagrodia, S., Forsburg, S. L. and Chernoff, J. (1995). Fission yeast pak1+ encodes a protein kinase that interacts with Cdc42p and is involved in the control of cell polarity and mating. *EMBO J.* **14**, 5908-5919. doi:10.1002/j.1460-2075.1995.tb00278.x

Pham, K., Shimoni, R., Charnley, M., Ludford-Menting, M. J., Hawkins, E. D., Ramsbottom, K., Oliaro, J., Izon, D., Ting, S. B., Reynolds, J. et al. (2015). Asymmetric cell division during T cell development controls downstream fate. *J. Cell Biol.* **210**, 933-950. doi:10.1083/jcb.201502053

Pöhlmann, J. and Fleig, U. (2010). Asp1, a conserved 1/3 inositol polyphosphate kinase, regulates the dimorphic switch in Schizosaccharomyces pombe. *Mol. Cell. Biol.* **30**, 4535-4547. doi:10.1128/MCB.00472-10

Prevorovsky, M., Stanurova, J., Puta, F. and Folk, P. (2009). High environmental iron concentrations stimulate adhesion and invasive growth of Schizosaccharomyces pombe. *FEMS Microbiol. Lett.* **293**, 130-134. doi:10.1111/j.1574-6968.2009.01515.x

Ren, L., Willet, A. H., Roberts-Galbraith, R. H., McDonald, N. A., Feoktistova, A., Chen, J.-S., Huang, H., Guillen, R., Boone, C., Sidhu, S. S. et al. (2015). The Cdc15 and Imp2 SH3 domains cooperatively scaffold a network of proteins that redundantly ensure efficient cell division in fission yeast. *Mol. Biol. Cell* **26**, 256-269. doi:10.1091/mbc.E14-10-1451

Rethinaswamy, A., Birnbaum, M. J. and Glover, C. V. C. (1998). Temperature-sensitive mutations of the CKA1 gene reveal a role for casein kinase II in maintenance of cell polarity in Saccharomyces cerevisiae. *J. Biol. Chem.* **273**, 5869-5877. doi:10.1074/jbc.273.10.5869

Roberts-Galbraith, R. H., Chen, J.-S., Wang, J. and Gould, K. L. (2009). The SH3 domains of two PCH family members cooperate in assembly of the Schizosaccharomyces pombe contractile ring. *J. Cell Biol.* **184**, 113-127. doi:10.1083/jcb.200806044

Robertson, A. M. and Hagan, I. M. (2008). Stress-regulated kinase pathways in the recovery of tip growth and microtubule dynamics following osmotic stress in S. pombe. *J. Cell Sci.* **121**, 4055-4068. doi:10.1242/jcs.034488

Sanchez-Diaz, A., Marchesi, V., Murray, S., Jones, R., Pereira, G., Edmondson, R., Allen, T. and Labib, K. (2008). Inn1 couples contraction of the actomyosin ring to membrane ingression during cytokinesis in budding yeast. *Nat. Cell Biol.* **10**, 395-406. doi:10.1038/ncb1701

Schindelin, J., Arganda-Carreras, I., Frise, E., Kaynig, V., Longair, M., Pietzsch, T., Preibisch, S., Rueden, C., Saalfeld, S., Schmid, B. et al. (2012). Fiji: an open-source platform for biological-image analysis. *Nat. Methods* **9**, 676-682. doi:10.1038/nmeth.2019

Shimada, Y., Gulli, M.-P. and Peter, M. (2000). Nuclear sequestration of the exchange factor Cdc24 by Far1 regulates cell polarity during yeast mating. *Nat. Cell Biol.* **2**, 117-124. doi:10.1038/35000073

Sipiczki, M., Takeo, K. and Grallert, A. (1998). Growth polarity transitions in a dimorphic fission yeast. *Microbiology* **144**, 3475-3485. doi:10.1099/00221287-144-12-3475

Snell, V. and Nurse, P. (1994). Genetic analysis of cell morphogenesis in fission yeast–a role for casein kinase II in the establishment of polarized growth. *EMBO J.* **13**, 2066-2074. doi:10.1002/j.1460-2075.1994.tb06481.x

Streiblova, E. and Wolf, A. (1972). Cell wall growth during the cell cycle of Schizosaccharomyces pombe. *Z. Allg. Mikrobiol.* **12**, 673-684.

Sudbery, P. E. (2011). Growth of Candida albicans hyphae. *Nat. Rev. Microbiol.* **9**, 737-748. doi:10.1038/nrmicro2636

Wach, A., Brachat, A., Pöhlmann, R. and Philippsen, P. (1994). New heterologous modules for classical or PCR-based gene disruptions in Saccharomyces cerevisiae. *Yeast* **10**, 1793-1808. doi:10.1002/yea.320101310

Yoon, H.-J., Feoktistova, A., Chen, J.-S., Jennings, J. L., Link, A. J. and Gould, K. L. (2006). Role of Hcn1 and its phosphorylation in fission yeast anaphase-promoting complex/cyclosome function. *J. Biol. Chem.* **281**, 32284-32293. doi:10.1074/jbc.M603867200

A

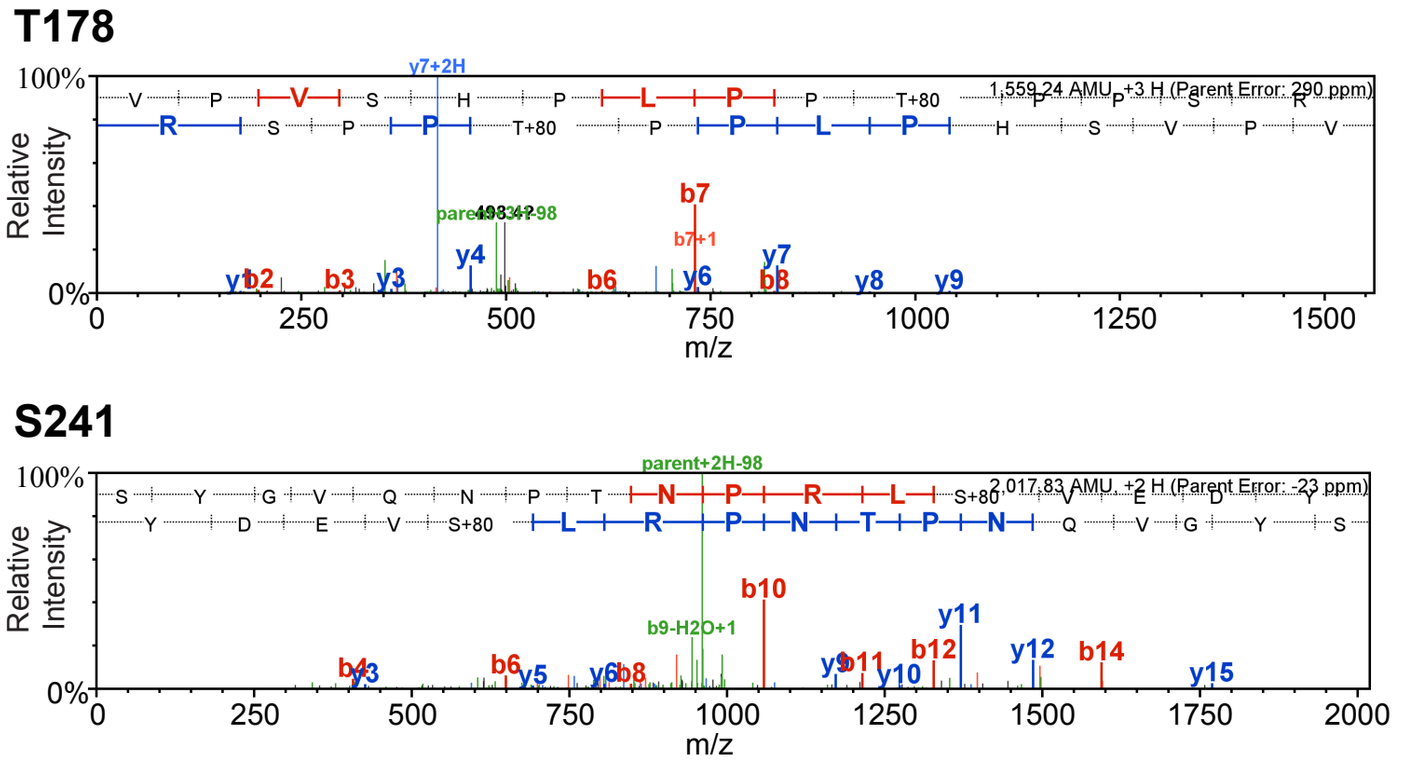

B

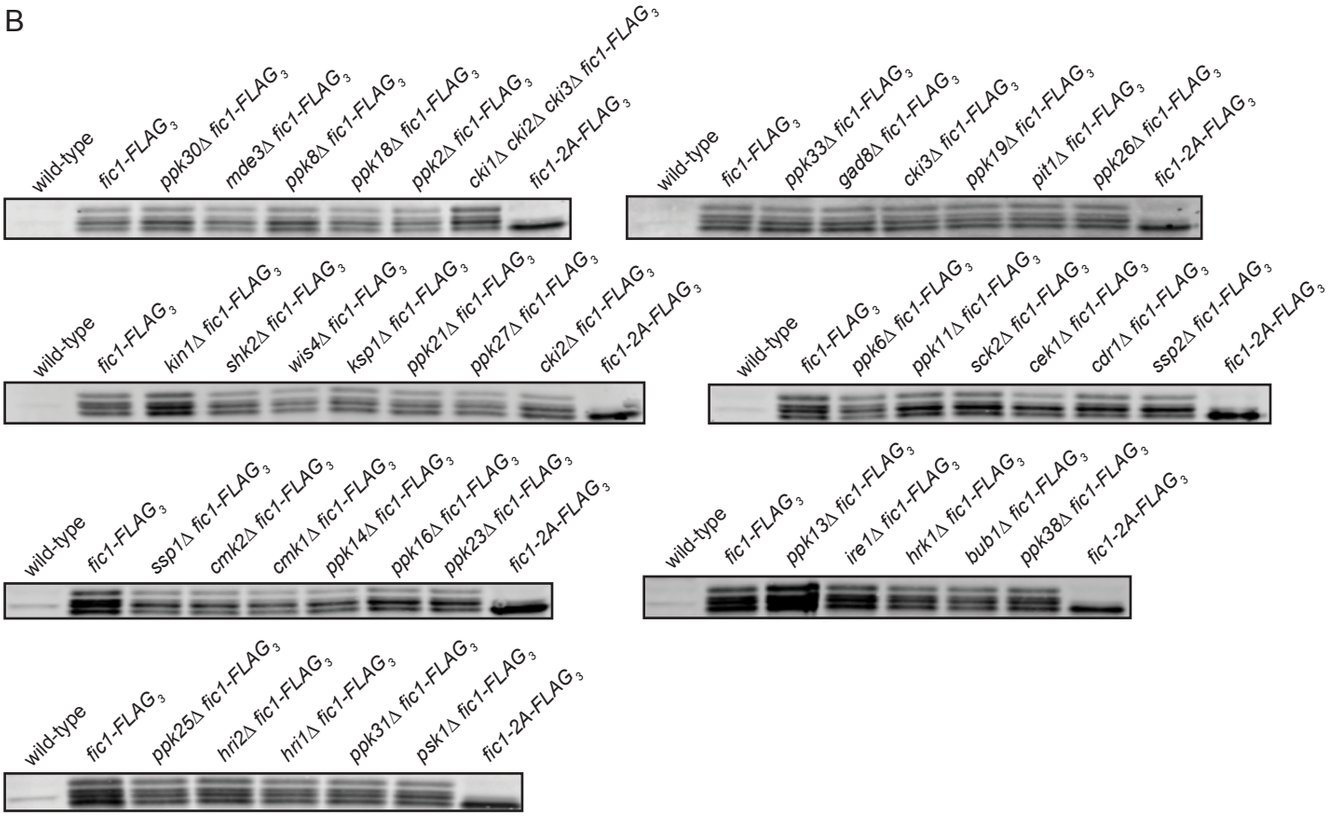

Figure S1

Figure S1. Fic1 residues T178 and S241 are phosphorylated *in vivo*. A) Representative MS2 spectra of peptides with phosphorylated T178 or S241, respectively, identified from Fic1-TAP affinity purifications. The peptide sequence ladder depicts y (colored blue) and b (colored red) ions of the peptide. Green peaks indicate either neutral loss of phosphate from the parent ions or loss of water from the fragmented product ions. Black peaks represent unidentified ions. B) Lysates from asynchronous cells of the indicated strains producing Fic1-$FLAG_3$ were immunoblotted for FLAG. In each panel, an untagged strain, a tagged strain with no kinase deletions, and Fic1-2A-$FLAG_3$ served as controls.

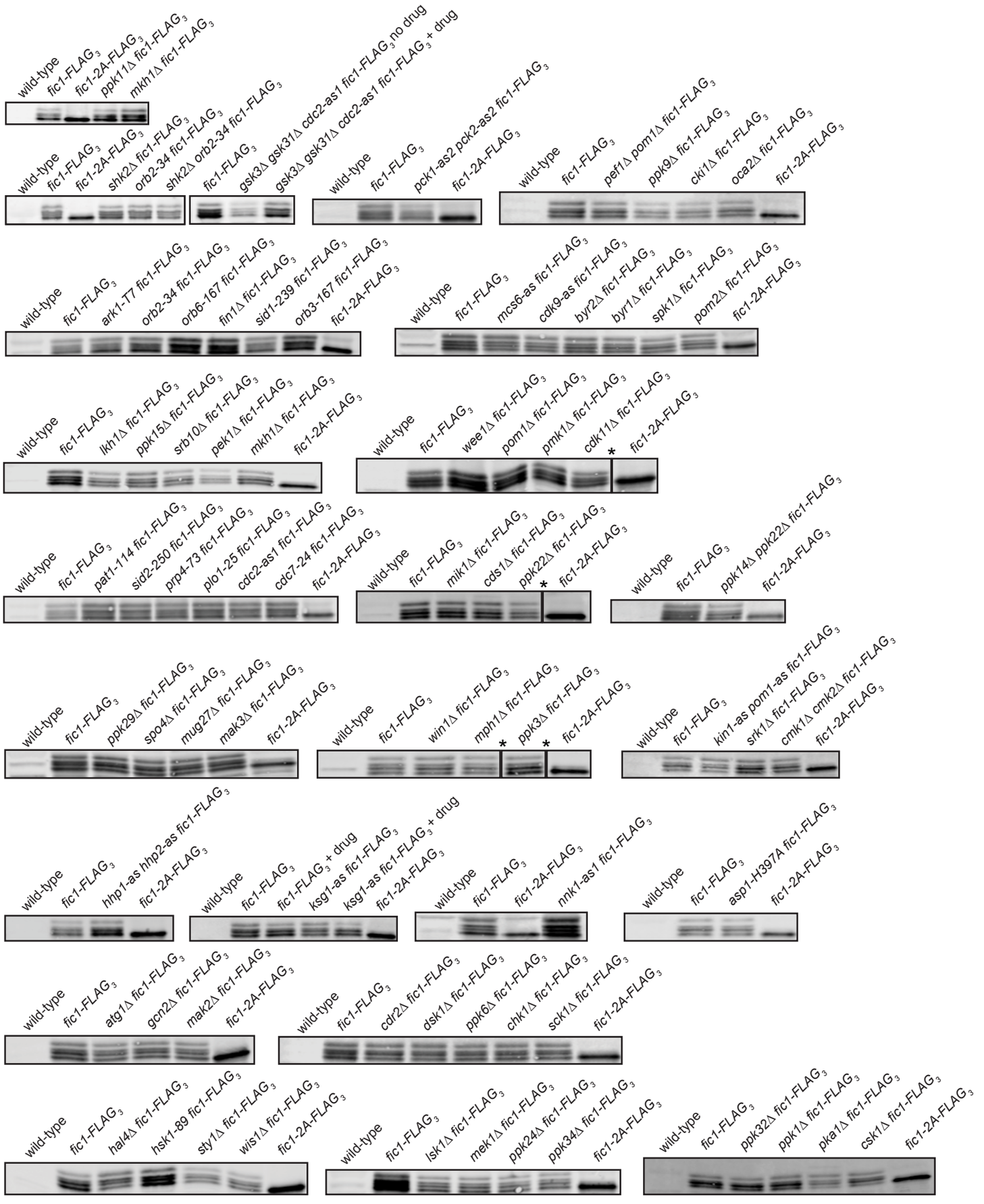
wild-type
fic1-FLAG3
fic1-2A-FLAG3
ppk11Δ fic1-FLAG3
mkh1Δ fic1-FLAG3
shk2Δ fic1-FLAG3
orb2-34 fic1-FLAG3
shk2Δ orb2-34 fic1-FLAG3
gsk3Δ gsk31Δ cdc2-as1 fic1-FLAG3 no drug
gsk3Δ gsk31Δ cdc2-as1 fic1-FLAG3 + drug
pck1-as2 pck2-as2 fic1-FLAG3
pef1Δ pom1Δ fic1-FLAG3
ppk9Δ fic1-FLAG3
cki1Δ fic1-FLAG3
oca2Δ fic1-FLAG3
ark1-T7 fic1-FLAG3
orb6-167 fic1-FLAG3
fin1Δ fic1-FLAG3
sid1-239 fic1-FLAG3
orb3-167 fic1-FLAG3
mcs6-as fic1-FLAG3
cdk9-as fic1-FLAG3
byr2Δ fic1-FLAG3
byr1Δ fic1-FLAG3
spk1Δ fic1-FLAG3
pom2Δ fic1-FLAG3
lkh1Δ fic1-FLAG3
ppk15Δ fic1-FLAG3
srb10Δ fic1-FLAG3
pek1Δ fic1-FLAG3
mkh1Δ fic1-FLAG3
wee1Δ fic1-FLAG3
pom1Δ fic1-FLAG3
pmk1Δ fic1-FLAG3
cdk11Δ fic1-FLAG3
pat1-114 fic1-FLAG3
sid2-250 fic1-FLAG3
prp4-73 fic1-FLAG3
plo1-25 fic1-FLAG3
cdc2-as1 fic1-FLAG3
cdc7-24 fic1-FLAG3
mik1Δ fic1-FLAG3
cds1Δ fic1-FLAG3
ppk22Δ fic1-FLAG3
ppk14Δ ppk22Δ fic1-FLAG3
ppk29Δ fic1-FLAG3
spo4Δ fic1-FLAG3
mug27Δ fic1-FLAG3
mak3Δ fic1-FLAG3
win1Δ fic1-FLAG3
mph1Δ fic1-FLAG3
ppk3Δ fic1-FLAG3
kin1-as pom1-as fic1-FLAG3
srk1Δ fic1-FLAG3
cmk1Δ cmk2Δ fic1-FLAG3
hhp1-as hhp2-as fic1-FLAG3
fic1-FLAG3 + drug
ksg1-as fic1-FLAG3
ksg1-as fic1-FLAG3 + drug
nnk1-as1 fic1-FLAG3
asp1-H397A fic1-FLAG3
atg1Δ fic1-FLAG3
gcn2Δ fic1-FLAG3
mak2Δ fic1-FLAG3
cdr2Δ fic1-FLAG3
dsk1Δ fic1-FLAG3
ppk6Δ fic1-FLAG3
chk1Δ fic1-FLAG3
sck1Δ fic1-FLAG3
hal4Δ fic1-FLAG3
hsk1-89 fic1-FLAG3
sty1Δ fic1-FLAG3
wis1Δ fic1-FLAG3
lsk1Δ fic1-FLAG3
mek1Δ fic1-FLAG3
ppk24Δ fic1-FLAG3
ppk34Δ fic1-FLAG3
ppk32Δ fic1-FLAG3
ppk1Δ fic1-FLAG3
pka1Δ fic1-FLAG3
csk1Δ fic1-FLAG3
fic1-2A-FLAG3

Figure S2

Figure S2. Fic1 phosphorylation is regulated by multiple kinases. Lysates from asynchronous cells of the indicated strains producing Fic1-FLAG$_3$ were immunoblotted for FLAG. In each panel, an untagged strain, a tagged strain with no kinase deletions, and Fic1-2A-FLAG$_3$ served as controls. For temperature-sensitive kinase strains, cells were shifted to 36˚C from 2 to 4 hours prior to lysis. For analog-sensitive strains, cells were treated with either 1-NM-PP1 (1 μM *cdc2-as1,* 25 μM *hhp1-as,* 25μM *hhp2-as*), 3-BrB-PP1 (30 μM *pck1-as2*, 30 μM *pck2-as2,* 30 μM *mcs6-as*), or 3-MB-PP1 (40 μM *cdk9-as,* 30 μM *ksg1-as,* 15 μM *kin1-as,* 15 μM *pom1-as*) for 30 min prior to lysis. Four asterisks (*) indicate where 4 lanes were cropped out of gel images.

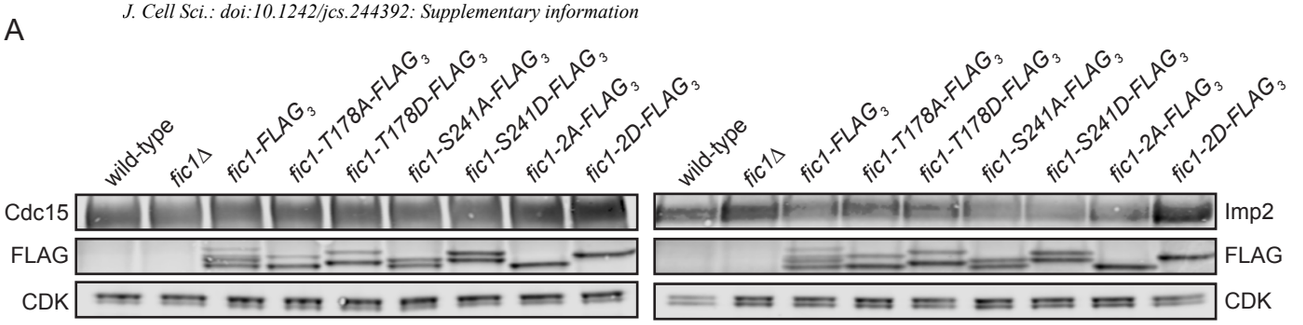

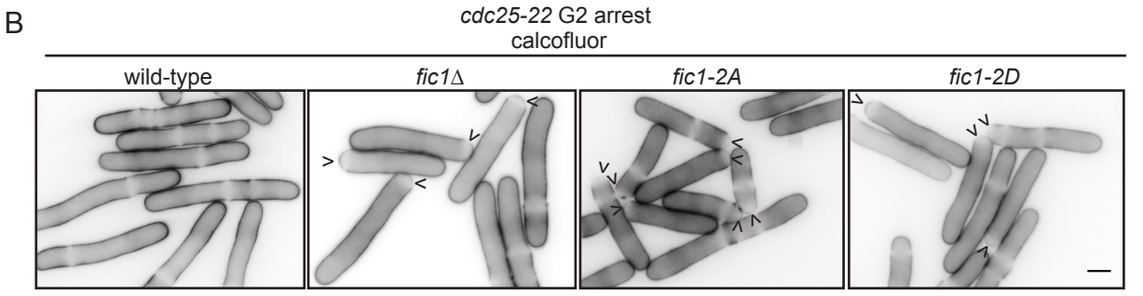

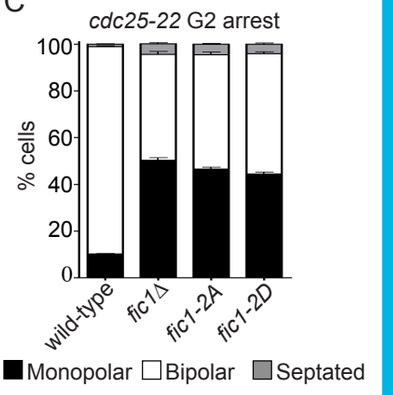

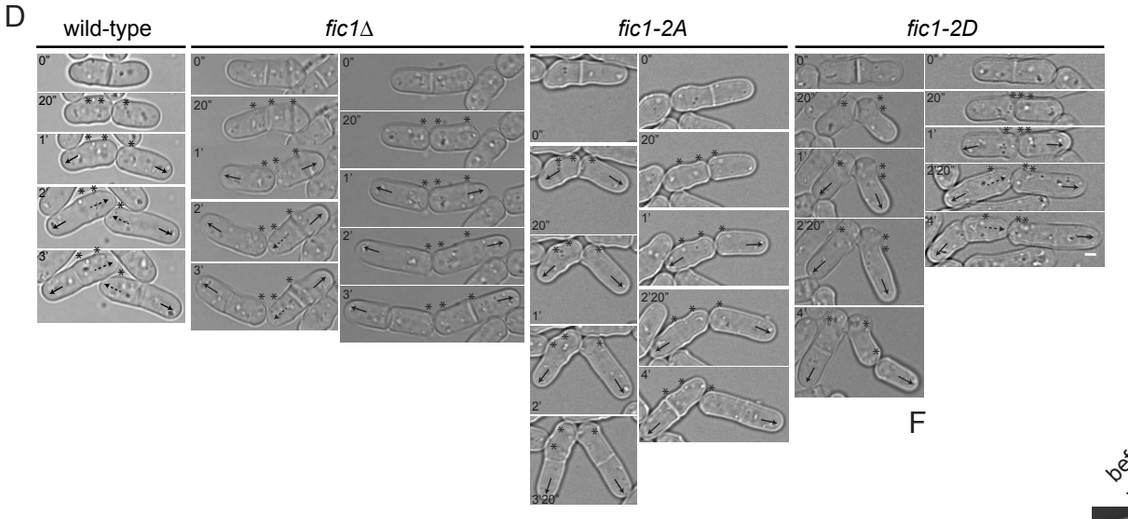

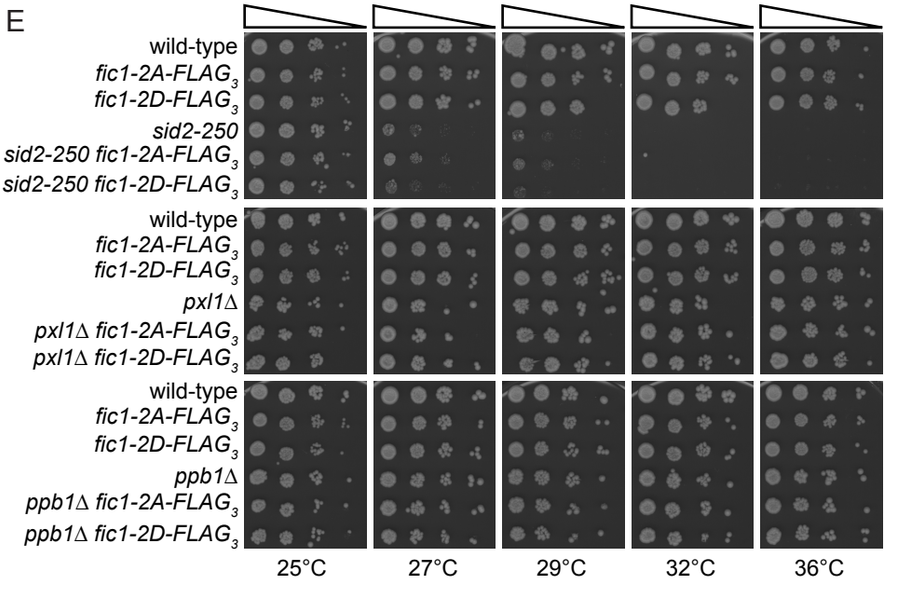

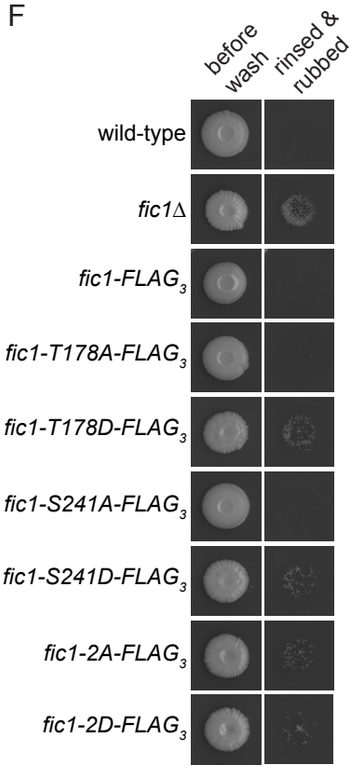

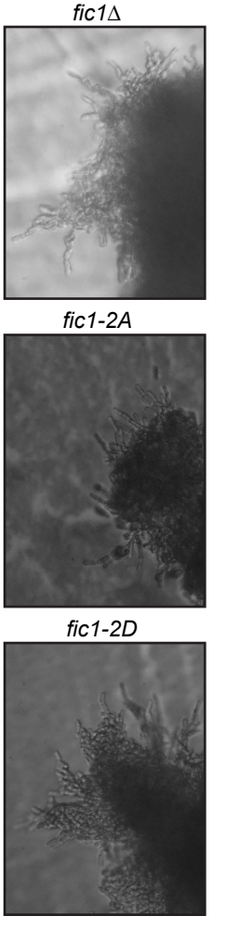

Figure S3

Figure S3. Deregulation of Fic1 phosphorylation at T178 an S241 impairs new end growth. A) Anti-Cdc15 or anti-Imp2 immunoprecipitates from cells of indicated genotypes were blotted with an anti-FLAG, anti-Cdc15, or anti-Imp2 antibody. Lysate samples were blotted with anti-CDK (PSTAIRE) as a control for input into the immunoprecipitations. B) Live-cell images of G2-arrested, calcofluor-stained cells of the indicated genotypes. Arrowheads indicate monopolar cells. Scale bar, 5 μm. C) Quantification of growth polarity phenotypes for G2-arrested cells of the indicated genotypes. Data from three trials per genotypes and n>200 for each trial are presented as mean ± SEM. D) Live-cell DIC movies of cells of the indicated genotypes. Solid arrows denote old end growth, whereas dashed arrows indicate new end growth. Birth scars are marked by asterisks. Time points are noted. Scale bar, 2 μm. E) Serial 1:10 dilutions of the indicated genotypes were spotted onto rich medium and incubated at the indicated temperatures. F) Invasive growth assays for strains of the indicated genotypes on 2% agar. Cells were spotted on rich medium and incubated for 20 days at 29°C (left panel). Colonies were then rinsed under a stream of water and rubbed off (right panel). G) Images of pseudohyphae for the genotypes indicated.

TABLE S1 *S. pombe* strains used in this study

Figure 1		
KGY246	*ade6-M210 ura4-D18 leu1-32 h⁻*	Lab Stock
KGY6288	*fic1-FLAG$_3$:kan^R ade6-M216 ura4-D18 leu1-32 h⁻*	Lab stock
KGY11409	*fic1-FLAG$_3$:kan^R cdc10-V50 ade6-M21X ura4-D18 leu1-32 h⁻*	This study
KGY6659	*fic1-FLAG$_3$:kan^R cdc25-22 ade6-M21X ura4-D18 leu1-32 h⁻*	This study
KGY7125	*fic1-FLAG$_3$:kan^R nda3-KM311 ade6-M21X ura4-D18 leu1-32 h⁻*	This study
KGY11422	*fic1-FLAG$_3$:kan^R cps1-191 lys1-131 ade6-M21X ura4-D18 leu1-32 h⁻*	This study
Figure 2		
KGY11242	*fic1(aa1-126)-GFP:kan^R ade6-M21X ura4-D18 leu1-32 h⁺*	This study
KGY11313	*fic1(aa127-End)-GFP:kan^R ade6-M21X ura4-D18 leu1-32 h⁺*	This study
KGY11309	*fic1-GFP:kan^R cdc15-mCherry:kan^R ade6-M21X ura4-D18 leu1-32 h⁻*	This study
KGY11280	*fic1-K22,27A-GFP:kan^R cdc15-mCherry:kan^R ade6-M21X ura4-D18 leu1-32 h⁻*	This study
KGY11152	*fic1-K22,27A ade6-M21X ura4-D18 leu1-31 h⁻*	This study
KGY11230	*fic1-K22,27A-FLAG$_3$:kan^R ade6-M210 ura4-D18 leu1-32 h⁻*	This study
KGY6678	*fic1::ura4⁺ ade6-M21X ura4-D18 leu1-32 h⁻*	Lab stock
KGY11858	*fic1-K22,27A-GFP:kan^R cdc15-mCherry:kan^R sid4-GFP:kan^R ade6-M21X ura4-D18 leu1-32 h⁻*	This study
Figure 3		
KGY11739	*fic1-T178A-FLAG$_3$:kan^R ade6-M21X ura4-D18 leu1-32 h⁻*	This study
KGY11908	*fic1-T178D-FLAG$_3$:kan^R ade6-M21X ura4-D18 leu1-32 h⁺*	This study
KGY11718	*fic1-S241A-FLAG$_3$:kan^R ade6-M21X ura4-D18 leu1-32 h⁻*	This study
KGY11854	*fic1-S241D-FLAG$_3$:kan^R ade6-M21X ura4-D18 leu1-32 h⁺*	This study
KGY11856	*fic1-T178A,S241A-FLAG$_3$:kan^R ade6-M21X ura4-D18 leu1-32 h⁺*	This study
KGY11861	*fic1-T178D,S241D-FLAG$_3$:kan^R ade6-M21X ura4-D18 leu1-32 h⁺*	This study
KGY849-2	*cdc2-F84G fic1-FLAG$_3$:hyg^R ade6-M21X ura4-D18 leu1-32 h⁻*	This study
KGY11546	*orb5-19 fic1-FLAG$_3$:kan^R ura4-D18 leu1-32 ade-M21X h?*	This study
KGY649-2	*cdc2-as1 orb5-19 fic1-FLAG$_3$:kan^R h⁺*	This study
Figure 4		
KGY731-3	*fic1-mNeonGreen:kan^R sad1-mCherry:nat^R ade6-M210 ura4-D18 leu1-32 h⁺*	This study

KGY357-2	*fic1-T178A,S241A-mNeonGreen:kan^R sad1-mCherry:nat^R ade6-M210 ura4-D18 leu1-32 h$^+$*	This study
KGY1757-2	*fic1-T178D,S241D-mNeonGreen:kan^R sad1-mCherry:nat^R ade6-M210 ura4-D18 leu1-32 h$^+$*	This study
KGY1507-2	*fic1-mNeonGreen:kan^R sad1-mNeonGreen:hyg^R ade6-M210 ura4-D18 leu1-32 h$^-$*	This study
KGY1609-2	*fic1-T178A,S241A-mNeonGreen:kan^R sad1-mNeonGreen:hyg^R ade6-M210 ura4-D18 leu1-32 h$^+$*	This study
KGY1726-2	*fic1-T178D,S241D-mNeonGreen:kan^R sad1-mNeonGreen:hyg^R ade6-M210 ura4-D18 leu1-32 h$^+$*	This study
Figure S1		
KGY6744	*fic1-TAP:kan^R ade6-M210 ura4-D18 leu1-32 h$^-$*	This study
KGY11444	*cmk2::ura4$^+$ fic1-FLAG$_3$:kan^R ade6-M21X ura4-D18 leu1-32 h$^-$*	This study
KGY11446	*cmk1::ura4$^+$ fic1-FLAG$_3$:kan^R ade6-M21X ura4-D18 leu1-32 h$^-$*	This study
KGY11458	*ppk16::ura4+ fic1-FLAG$_3$:kan^R ade6-M210 ura4-D18 leu1-32 h-*	This study
KGY16194	*ppk2::ura4$^+$ fic1-FLAG$_3$:kan^R ura4-D18 leu1-32 ade6-M21X h$^+$*	This study
KGY11460	*ppk23::ura4$^+$ fic1-FLAG$_3$:kan^R leu1-32 ura4-D18 h$^-$*	This study
KGY11475	*cek1::ura4$^+$ fic1-FLAG$_3$:kan^R ura4-D18 leu1-32 ade6-M210 h$^-$*	This study
KGY11469	*ppk11:ura4$^+$ fic1-FLAG$_3$:kan^R ura4-D18 leu1-32 h$^+$*	This study
KGY11457	*ppk14::ura4$^+$ fic1-FLAG$_3$:kan^R ura4-D18 leu1-32 ade6-M21X h$^-$*	This study
KGY11473	*sck2::ura4$^+$ fic1-FLAG$_3$:kan^R h$^+$*	This study
KGY578-2	*ssp1::ura4$^+$ fic1-FLAG$_3$:kan^R leu1-32 ura4-D18 h$^+$*	This study
KGY14415	*ssp2::kan^R fic1-FLAG$_3$:kan^R ura4-D18 leu1-32 ade6-M21X h$^+$*	This study
KGY13645	*fic1-FLAG$_3$:kan^R wis4::kan^R ura4-D18 leu1-32 ade6-M21X h$^-$*	This study
KGY13858	*bub1::kan^R fic1-FLAG$_3$:hyg^R ura4-D18 leu1-32 ade6-M21X h$^+$*	This study
KGY11476	*cdr1::ura4$^+$ fic1-FLAG$_3$:kan^R ura4-D18 leu1-32 ade6-M21X h$^-$*	This study
KGY13881	*cki2::kan^R fic1-FLAG$_3$:hyg^R ura4-D18 leu1-32 ade6-M21X h$^+$*	This study
KGY14417	*cki3::ura4$^+$ fic1-FLAG$_3$:kan^R h$^-$*	This study
KGY15136-2	*cki1::kan^R cki2::ura4$^+$ cki3::ura4$^+$ fic1-FLAG$_3$:kan^R ura4-D18 leu1-32 h$^+$*	This study
KGY14416	*gad8::ura4$^+$ fic1-FLAG$_3$:kan^R ura4-D18 leu1-32 ade6-M21X h$^+$*	This study
KGY13850	*hri1::kan^R fic1-FLAG$_3$:hyg^R ura4-D18 leu1-32 ade6-M21X h$^+$*	This study

KGY13849	*hri2::kan^R fic1-FLAG$_3$:hyg^R ura4-D18 leu1-32 ade6-M21X h$^+$*	This study
KGY13836	*hrk1::kan^R fic1-FLAG$_3$:hyg^R ura4-D18 leu1-32 ade6-M21X h$^+$*	This study
KGY13831	*ire1::kan^R fic1-FLAG$_3$:hyg^R ura4-D18 leu1-32 ade6-M21X h$^+$*	This study
KGY2326-2	*kin1::ura4$^+$ fic1-FLAG$_3$:kan^R ura4-D18 leu1-32 ade6-M21X h$^+$*	This study
KGY13844	*ksp1::kan^R fic1-FLAG$_3$:hyg^R ura4-D18 leu1-32 ade6-M21X h$^+$*	This study
KGY13839	*mde3::kan^R fic1-FLAG$_3$:hyg^R ura4-D18 leu1-32 ade6-M21X h$^+$*	This study
KGY15977	*pit1::ura4$^+$ fic1-FLAG$_3$:kan^R ade6-M210 ura4-D18 leu1-32 h$^-$*	This study
KGY13837	*ppk13::kan^R fic1-FLAG$_3$:hyg^R ura4-D18 leu1-32 ade6-M21X h$^+$*	This study
KGY15135-2	*ppk18::ura4$^+$ fic1-FLAG$_3$:kan^R ura4-D18 leu1-32 h$^-$*	This study
KGY15976	*ppk19::ura4$^+$ fic1-FLAG$_3$:kan^R ade6-M210 ura4-D18 leu1-32 h$^-$*	This study
KGY13846	*ppk21::kan^R fic1-FLAG$_3$:hyg^R ura4-D18 leu1-32 ade6-M21X h$^+$*	This study
KGY13845	*ppk25::kan^R fic1-FLAG$_3$:hyg^R ura4-D18 leu1-32 ade6-M21X h$^+$*	This study
KGY16196	*ppk26::ura4$^+$ fic1-FLAG$_3$:kan^R ura4-D18 leu1-32 ade6-M21X h$^-$*	This study
KGY13848	*ppk27::kan^R fic1-FLAG$_3$:hyg^R ura4-D18 leu1-32 ade6-M21X h$^+$*	This study
KGY15137-2	*ppk30::ura4$^+$ fic1-FLAG$_3$:kan^R ade6-M210 ura4-D18 leu1-32 h$^-$*	This study
KGY13859	*ppk31::kan^R fic1-FLAG$_3$:hyg^R ura4-D18 leu1-32 ade6-M21X h$^+$*	This study
KGY14414	*ppk33::ura4$^+$ fic1-FLAG$_3$:kan^R leu1-32 h$^+$*	This study
KGY14291	*ppk38::ura4$^+$ fic1-FLAG$_3$:hyg^R ade6-M210 ura4-D18 leu1-32 h$^-$*	This study
KGY11462	*ppk6::ura4$^+$ fic1-FLAG$_3$:kan^R h$^-$*	This study
KGY13851	*ppk8::kan^R fic1-FLAG$_3$:hyg^R ura4-D18 leu1-32 ade6-M21X h$^+$*	This study
KGY13884	*psk1::kan^R fic1-FLAG$_3$:hyg^R ura4-D18 leu1-32 ade6-M21X h$^+$*	This study
KGY11961	*shk2::ura4$^+$ fic1-FLAG$_3$:kan^R ura4D18 leu1-32 h$^+$*	This study
Figure S2		
KGY11623	*ark1-T7:kan^R fic1-FLAG$_3$:kan^R ade6-M21X ura4-D18 leu1-32 h$^+$*	This study
KGY849-2	*cdc2-F84G fic1-FLAG$_3$:hyg^R ade6-M21X ura4-D18 leu1-32 h$^-$*	This study

KGY11626	*cdc7-24 fic1-FLAG$_3$:kan^R ura4-D18 leu1-32 ade6-M21X h$^-$*	This study
KGY14413	*fin1::ura4$^+$ fic1-FLAG$_3$:kan^R ura4-D18 leu1-32 ade6-M21X h$^-$*	This study
KGY14421	*pat1-114 fic1-FLAG$_3$:kan^R ura4-D18 leu1-32 ade6-M21X h$^+$*	This study
KGY11624	*sid1-239 fic1-FLAG$_3$:kan^R ura4-D18 leu1-32 ade6-M21X h$^-$*	This study
KGY14425	*sid2-250 fic1-FLAG$_3$:kan^R ura4-D18 leu1-32 ade6-M21X h$^+$*	This study
KGY18170	*nnk1-as2(M537A)-HA-TAP:kan^R fic1-FLAG$_3$:kanR h$^+$*	This study
KGY14422	*prp4-73 fic1-FLAG$_3$:kan^R ura4-D18 leu1-32 h$^+$*	This study
KGY11628	*plo1-25 fic1-FLAG$_3$:kan^R h$^-$*	This study
KGY14420	*orb6-167 fic1-FLAG$_3$:kan^R ura4-D18 leu1-32 h$^-$*	This study
KGY16437-2	*cdk9-as fic1-FLAG$_3$:hyg^R h$^+$*	This study
KGY11968	*orb3-167 fic1-FLAG$_3$:kan^R ura4-D18 leu1-32 ade6-M21X h$^-$*	This study
KGY11405	*orb2-34 fic1-FLAG$_3$:kan^R ura4-D18 leu1-32 ade6-M21X h$^-$*	This study
KGY17133	*pck1-as2-HA:hyg^R pck2-as2-HA:hyg^R fic1-FLAG$_3$:kan^R h$^+$*	This study
KGY980-2	*gsk3::ura4$^+$ gsk31::kan^R cdc2-F84G fic1-FLAG$_3$:hyg^R ade6-M21X ura4-D18 leu1-32 h$^-$*	This study
KGY19510	*hhp1-as(M84G):kan^R hhp2-as(M85G):nat^R fic1-FLAG$_3$:hyg^R ura4-D18 leu1-32 ade6-M21X h$^-$*	This study
KGY19814	*hal4::kan^R fic1-FLAG$_3$:hyg^R ade6-M210 ura4-D18 leu1-32 h-*	This study
KGY11477	*lkh1::ura4+ fic1-FLAG$_3$:kan^R leu1-32 ura4-D18 h$^-$*	This study
KGY19689	*lsk1::kan^R fic1-FLAG$_3$:hyg^R ade6-M210 ura4-D18 leu1-32 h$^-$*	This study
KGY11960	*mkh1::ura4$^+$ fic1-FLAG$_3$:kan^R ura4-D18 leu1-32 ade6-M21X h$^+$*	This study
KGY11959	*pek1::ura4$^+$ fic1-FLAG$_3$:kan^R ura4-D18 leu1-32 ade6-M210 h$^+$*	This study
KGY1630-2	*pka1::kan^R fic1-FLAG$_3$:hyg^R ade6-M210 ura4-D18 leu1-32 h$^-$*	This study
KGY11443	*pmk1::ura4$^+$ fic1-FLAG$_3$:kan^R ura4-D18 leu1-32 ade6-M21X h$^-$*	This study
KGY11395	*pom1::ura4$^+$ fic1-FLAG$_3$:kan^R leu1-32 ura4-D18 h$^+$*	This study
KGY11479	*ppk15::ura4$^+$ fic1-FLAG$_3$:kan^R h$^+$*	This study
KGY11471	*ppk15::ura4$^+$ fic1-FLAG$_3$:kan^R leu1-32 ura4-D18 h$^+$*	This study
KGY19813	*sty1::kan^R fic1-FLAG:hyg^R ade6-M210 ura4-D18 leu1-32 h$^-$*	This study
KGY11392	*wee1::ura4$^+$ fic1-FLAG$_3$:kan^R leu1-32 ura4-D18 h$^-$*	This study

KGY19812	*wis1::kan^R fic1-FLAG$_3$:hyg^R ade6-M210 ura4-D18 leu1-32 h$^-$*	This study
KGY14258	*cmk1::ura4$^+$ cmk2::ura4+ fic1-FLAG$_3$:kan^R ura4D18 leu1-32 h$^-$*	This study
KGY11462	*ppk6::ura4$^+$ fic1-FLAG$_3$:kan^R h$^-$*	This study
KGY13636	*spk1::kan^R fic1-FLAG$_3$:hyg^R ura4-D18 leu1-32 ade6-M21X h$^+$*	This study
KGY13590	*win1::kan^R fic1-FLAG$_3$:kan^R ura4-D18 leu1-32 ade6-M21X h$^+$*	This study
KGY19716	*atg1::kan^R fic1-FLAG$_3$:hyg^R ade6-M210 ura4-D18 leu1-32 h$^-$*	This study
KGY13635	*byr1::kan^R fic1-FLAG$_3$:hyg^R ura4-D18 leu1-32 ade6-M21X h$^+$*	This study
KGY13633	*byr2::kan^R fic1-FLAG$_3$:hyg^R ura4-D18 leu1-32 ade6-M21X h$^+$*	This study
KGY2382-2	*cdr2::ura4$^+$ fic1-FLAG$_3$:hyg^R leu1-32 ura4-D18 h$^-$*	This study
KGY14185	*cki1::ura4$^+$ fic1-FLAG$_3$:kan^R ura4-D18 leu1-32 h-*	This study
KGY19686	*ppk34::kan^R fic1-FLAG$_3$:hyg^R ade6-M210 ura4-D18 leu1-32 h$^-$*	This study
KGY1872-2	*csk1::ura4$^+$ fic1-FLAG$_3$:hyg^R ura4-D18 leu1-32 ade6-M210 h$^-$*	This study
KGY13828	*dsk1::kan^R fic1-FLAG$_3$:hyg^R ura4-D18 leu1-32 ade6-M21X h$^+$*	This study
KGY19714	*gcn2::kan^R fic1-FLAG$_3$:hyg^R ade6-M210 ura4-D18 leu1-32 h$^-$*	This study
KGY19774	*hsk1-89:ura4$^+$ fic1-FLAG$_3$:hyg^R ura4-D18 leu1-32 h$^-$*	This study
KGY11720	*ksg1-as(L177G):hyg^R fic1-FLAG$_3$:kan^R leu1-32 ura4-D18 ade6-210 h$^-$*	This study
KGY19715	*mak2::kan^R fic1-FLAG$_3$:hyg^R ade6-M210 ura4-D18 leu1-32 h$^-$*	This study
KGY12756	*mak3::kan^R fic1-FLAG$_3$:hyg^R ura4-D18 leu1-32 ade6-M21X h$^+$*	This study
KGY16417	*mcs6-as fic1-FLAG$_3$:hyg^R ura4-D18 leu1-32 ade6-M21X h$^-$*	This study
KGY19688	*mek1::kan^R fic1-FLAG$_3$:hyg^R ade6-M210 ura4-D18 leu1-32 h$^-$*	This study
KGY13860	*mik1::kan^R fic1-FLAG$_3$:hyg^R ura4-D18 leu1-32 ade6-M21X h$^+$*	This study
KGY13861	*mph1::kan^R fic1-FLAG$_3$:hyg^R ura4-D18 leu1-32 ade6-M21X h$^+$*	This study
KGY12890	*mug27::kan^R fic1-FLAG$_3$:hyg^R ura4-D18 leu1-32 ade6-M21X h$^+$*	This study
KGY14201	*oca2::ura4$^+$ fic1-FLAG$_3$:kan^R ade6-M210 ura4-D18 leu1-32 h$^-$*	This study
KGY16000	*pef1::ura4$^+$ fic1-FLAG$_3$::kan^R ura4-D18 leu1-32 ade6-M21X h^{90}*	This study

KGY13826	*pom2::kan^R fic1-FLAG$_3$:hyg^R ura4-D18 leu1-32 ade6-M21X h$^+$*	This study
KGY1576-2	*ppk1::kan^R fic1-FLAG$_3$:hyg^R ura4-D18 leu1-32 ade6-M21X h$^+$*	This study
KGY13817-2	*ppk22::ura4$^+$ fic1-FLAG$_3$:kan^R ura4-D18 leu1-32 ade6-M21X h$^+$*	This study
KGY19687	*ppk24::kan^R fic1-FLAG$_3$:hyg^R ade6-M210 ura4-D18 leu1-32 h$^-$*	This study
KGY13863	*ppk29::kan^R fic1-FLAG$_3$:hyg^R ura4-D18 leu1-32 ade6-M21X h$^+$*	This study
KGY16195	*ppk3::ura4$^+$ fic1-FLAG$_3$:kan^R ura4-D18 leu1-32 ade6-M21X h$^-$*	This study
KGY1559-2	*ppk32::ura4$^+$ fic1-FLAG$_3$:hyg^R ura4-D18 leu1-32 h$^-$*	This study
KGY14186	*ppk9::ura4$^+$ fic1-FLAG$_3$:kan^R ade6-M21x leu1-32 ura4-D18 h$^-$*	This study
KGY13830	*sck1::kan^R fic1-FLAG$_3$:hyg^R ura4-D18 leu1-32 ade6-M21X h$^+$*	This study
KGY13056	*spo4::kan^R fic1-FLAG$_3$:hyg^R ura4-D18 leu1-32 ade6-M21X h$^+$*	This study
KGY13852	*srk1::kan^R fic1-FLAG$_3$:hyg^R ura4-D18 leu1-32 ade6-M21X h$^+$*	This study
KGY16425	*orb2-34 shk2::kan^R fic1-FLAG$_3$:hyg^R ura4-D18 leu1-32 ade6-M21X h$^+$*	This study
KGY13818-2	*pef1::ura4$^+$ pom1::ura4$^+$ fic1-FLAG$_3$:kan^R leu1-32 ura4-D18 h$^+$*	This study
KGY14256	*kin1-as-FLAG$_3$:kan^R pom1-as-tdTomato:nat^R fic1-FLAG:hyg^R leu1-32 ade6-M21X h$^+$*	This study
KGY649-2	*cdc2-as1 orb5-19 fic1-FLAG$_3$:kan^R h$^+$*	This study
KGY19605	*ppk14::ura4$^+$ ppk22::ura4$^+$ fic1-FLAG$_3$:hyg^R h$^-$*	This study
Figure S3		
KGY443	*cdc25-22 ade-M210 ura4-D18 leu1-32 h$^-$*	Lab stock
KGY10780	*fic1::ura4$^+$ cdc25-22 ade6-M210 ura4-D18 leu1-32 h$^-$*	This study
KGY13540	*fic1-T178A,S241A-FLAG$_3$:kan^R cdc25-22 ade6-M210 ura4-D18 leu1-32 h$^+$*	This study
KGY13541	*fic1-T178D,S241D-FLAG$_3$:kan^R cdc25-22 ade6-M210 ura4-D18 leu1-32 h$^-$*	This study
KGY1105	*sid2-250 ade6-21x ura4-D18 leu1-32 h$^-$*	Lab stock
KGY15374	*sid2-250 fic1-T178A,S241A-FLAG$_3$:kan^R ade6-M210 ura4-D18 leu1-32 h$^-$*	This study
KGY15374	*sid2-250 fic1-T178D,S241D-FLAG$_3$:kan^R ade6-M210 ura4-D18 leu1-32 h$^+$*	
KGY16851	*pxl1::ura4$^+$ ade6-M21X ura4-D18 leu1-32 h$^-$*	Lab stock
KGY1457-2	*pxl1::ura4$^+$ fic1-T178A,S241A-FLAG$_3$:kan^R ade6-M210 ura4-D18 leu1-32 h$^+$*	This study

KGY1458-2	*pxl1::ura4*$^{+}$ *fic1-T178D,S241D-FLAG*$_3$*:kan*^{R} *ade6-M210 ura4-D18 leu1-32 h*$^{-}$	This study
KGY1769-2	*ppb1::ura4*$^{+}$ *ade6-M210 ura4-D18 leu1-32 h*$^{-}$	Lab stock
KGY1465-2	*ppb1::ura4*$^{+}$ *fic1-T178A,S241A-FLAG*$_3$*:kan*^{R} *ade6-M210 ura4-D18 leu1-32 h*$^{-}$	This study
KGY1459-2	*ppb1::ura4*$^{+}$ *fic1-T178D,S241D-FLAG*$_3$*:kan*^{R} *ade6-M210 ura4-D18 leu1-32 h*$^{-}$	This study